Design Project of Lightweight Composite Structures

Kaya Onur Dag
s111058

Department of Wind Energy
Technical University of Denmark (DTU)
April 2013

Contents

List of Figures

List of Tables

Abstract

In this work, the aim was to make a blade which would be able to withstand under given loads.

At the beginning beam approach was conducted in which cap regions were designed and tested with panel buckling assumption and maximum strain and Tsai-Wu failure.

In the second part, the cap thicknesses were taken from the first part and implemented to the Becas software. With the rapidity of the Becas, behaviors were observed in different regions of the blade with varying materials and as well as their thicknesses.

After these steps, to design a blade which has enough buckling resistance, Abaqus software was used to conduct linear buckling analysis. It was observed that to design such a blade with iterations, a powerful computer was needed yet it was almost impossible to adjust the blade configuration and re-run the buckling simulation. Hence, it was difficult to gather intuitive understanding of buckling inclination for different material configurations inside problematic regions of the blade. As a result of this, a single blade became as heavy as a Vestas V90 3MW nacelle at the end. The total mass could easily be decreased yet this was not possible with current facilities.

At the very end, where buckling resistance was enough to handle the whole load, the frequency and maximum tip deflection check was done and the edgewise frequency was needed to be increased. For this purpose some unidirectional fibers were added in nose and tail regions and very last buckling check was done with Abaqus software on the last configuration with correct frequencies.

The configuration can be found in the TableB.1 in Appendix B and buckling response figures can be followed in AppendixC.

Chapter 1

Introduction

The structural blade design so far became important due to very much increased blade lengths. For a wind turbine blade, the structure which does the aerodynamic work is also employed to carry its self. Moreover, a perfect aerodynamic design may also not be the best choice from load carrying point of view. As a result of some application issues, there have been some restrictions being used on aerodynamic design such as maximum chord length, root section airfoil thicknesses and of course blade length. Due to excessive blade lengths for very large turbines, structural limits are reached and, on the other hand, the cost of the blade became an important issue due to trend in cheaper green energy.

In order to satisfy all these restrictions, the material configuration design becomes handy. Simply, the better layout would result as cheaper blades with low level aerodynamic sacrifices.

In this paper a structural material configuration of a 90 meter wind turbine blade is discussed in two different ways. In the first approach, blade is taken into account as if it only had cap regions and calculations are done with beam theory under a single load case. Afterwards, the BECAS and Abaqus software is used and a detailed design is proceeded.

Chapter 2

Turbine Blade as a Simple Beam

2.1 Theory

2.1.1 Total Deflection

Simply the moment curvature relation can be defined as shown in Eq.2.1 [4].

$$\frac{M_b}{EI} = \frac{\frac{d^2u}{dx^2}}{[1 + (\frac{du}{dx})^2]^{\frac{3}{2}}} \tag{2.1}$$

where u is the deflection due to bending. For small displacement and rotations, the equation can be written as Eq.2.2 .

$$\frac{M_b}{EI} = \frac{d^2u}{dx^2} \tag{2.2}$$

The right hand side of the equation can be called as *local curvature*. Double integration of this will result as total displacement for corresponding point due to applied bending moment. To take the integration, boundary conditions must be applied in order to find the integration constants which will pop up in each integration step.

The single beam is shown in Fig.2.1. The fixed part of the beam can provide two boundary conditions which are $\frac{du}{dx} = 0$ and $u(x) = 0$ on x_0.

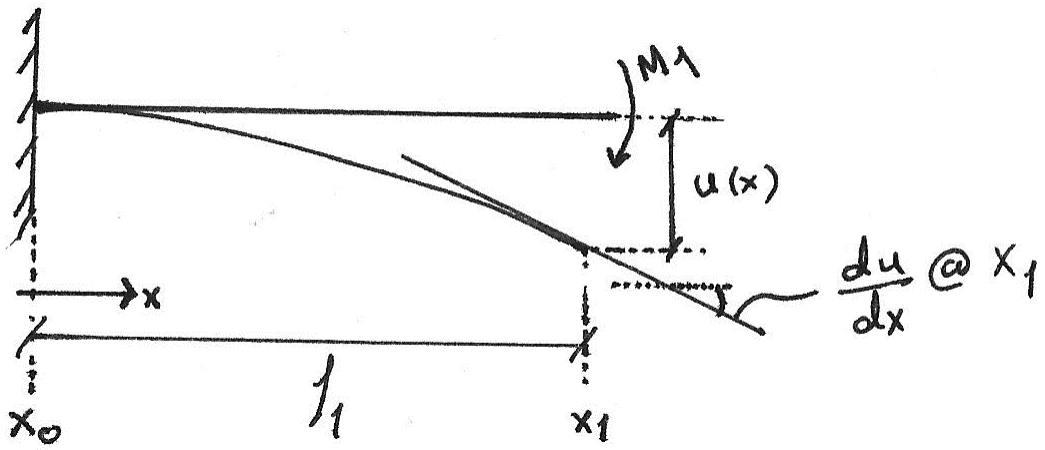

Figure 2.1: Single Beam

At the end, the deflection and the slope at the free end becomes:

$$u(x_1) = \frac{1}{2}\frac{M}{EI}l_1^2 \tag{2.3}$$

$$\frac{du}{dx} = \frac{M}{EI}l_1 \tag{2.4}$$

where l_1 is the distance between x_0 and x_1 and $\frac{du}{dx}$ or α is the slope at the point x_1.

For our case, the wind turbine blade is assumed to consist of caps and modeled as an I beam and without the mid connection region. Normally, the mid region of the I beams are employed to pass the shear to transfer the acting force as if it was a moment. Without the mid-connection, for a wind turbine blade section, the result would be only a pure bending of two different panels independently as shown in the left of the Fig2.2 and the cross-section would slide. However for our model, the load input already a moment distribution. As a result of this, there is no shear forces acting. In reality shear webs are employed to transfer the load. The simple cross-section drawing with a single web is shown in the right of the Fig.2.2.

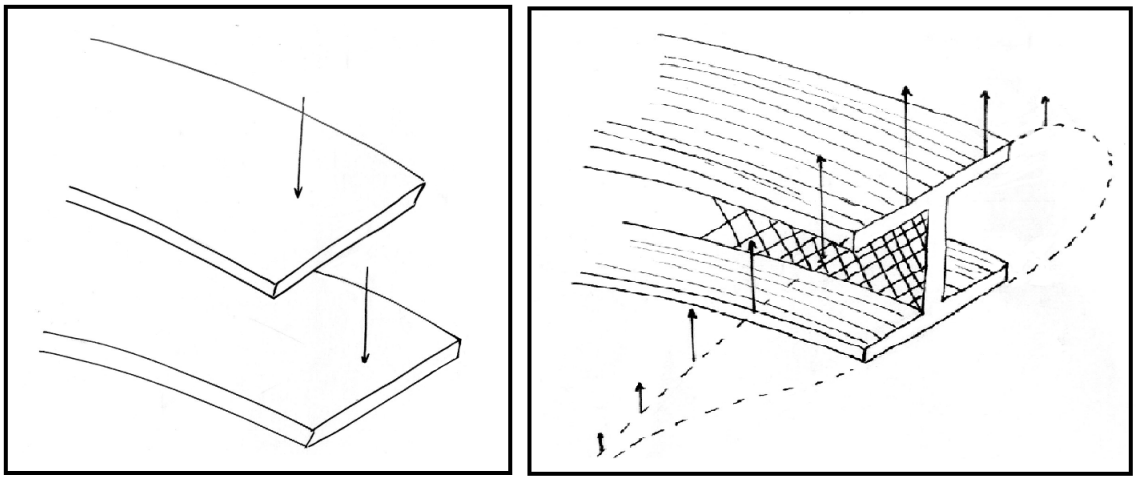

Figure 2.2: Two seperate beams under a force(left), an I beal as a wind turbine blade cross-section(right).

The whole beam has 5 sections where they connected upon each other. The details of the blade are shown in the Fig.2.3.

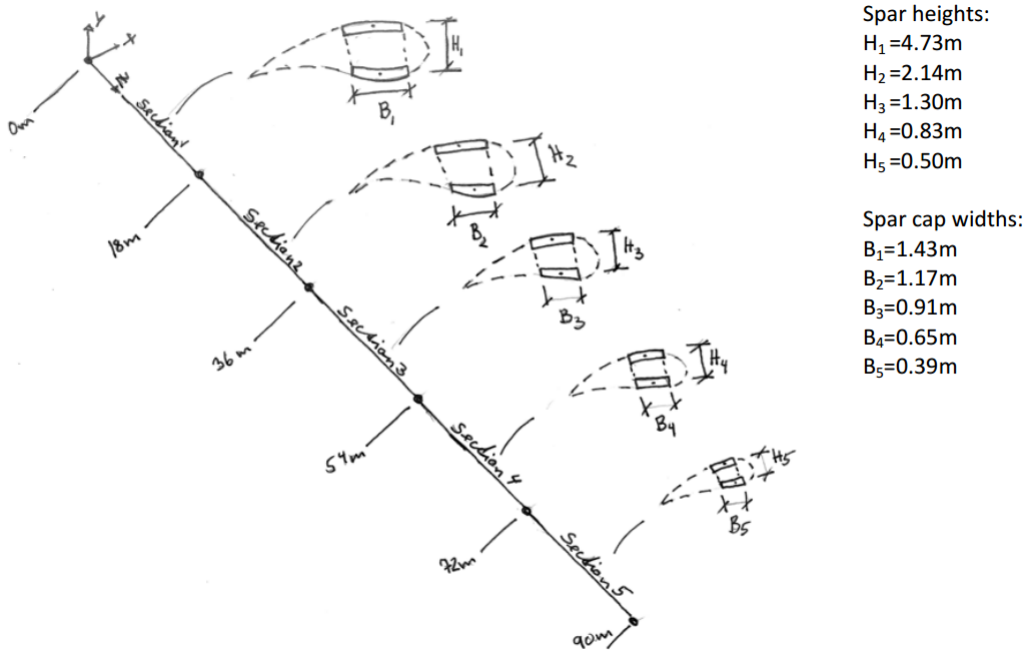

Figure 2.3: Definition of the blade [1]

The equations for deflections at each point are shown below.

$$u(18) = \frac{1}{2}\frac{M_1}{E_1 I_1} l_1^2 \tag{2.5}$$

$$\alpha(18) = \frac{M_1}{E_1 I_1} l_1 \tag{2.6}$$

For the next control point, which is 36^{th} meter for our beam, the slope at the point 18^{th} needs to taken into account.

$$u(36) = u(18) + l_2\alpha(18) + \frac{1}{2}\frac{M_2}{E_2 I_2} l_2^2 \tag{2.7}$$

$$\alpha(36) = \alpha(18) + \frac{M_2}{E_2 I_2} l_2 \tag{2.8}$$

$$u(54) = u(36) + l_3\alpha(36) + \frac{1}{2}\frac{M_3}{E_3 I_3} l_3^2 \tag{2.9}$$

$$\alpha(54) = \alpha(36) + \frac{M_3}{E_3 I_3} l_3 \tag{2.10}$$

$$u(72) = u(54) + l_4\alpha(54) + \frac{1}{2}\frac{M_4}{E_4 I_4} l_4^2 \tag{2.11}$$

$$\alpha(72) = \alpha(54) + \frac{M_4}{E_4 I_4} l_4 \tag{2.12}$$

$$u(90) = u(72) + l_4\alpha(72) + \frac{1}{2}\frac{M_5}{E_5 I_5} l_5^2 \tag{2.13}$$

$$\alpha(90) = \alpha(72) + \frac{M_5}{E_5 I_5} l_5 \tag{2.14}$$

All of these steps are provided inside the Matlab code in AppendixA.1 between the lines 51 and 64.

For our case E and moment of inertia I are calculated as shown below.

$$E = \frac{A_{11}(1 - \nu_{12}\nu_{21})}{t} \tag{2.15}$$

$$I = (\frac{1}{12}Bt^3 + (tB)(\frac{H-t}{2})^2)2 \tag{2.16}$$

Where A_{11} is from the ABD matrix.

2.1.2 Stresses

The moment on each section represented as compression and tensile forces on z-axis. The detailed description is shown in the Fig.2.4.

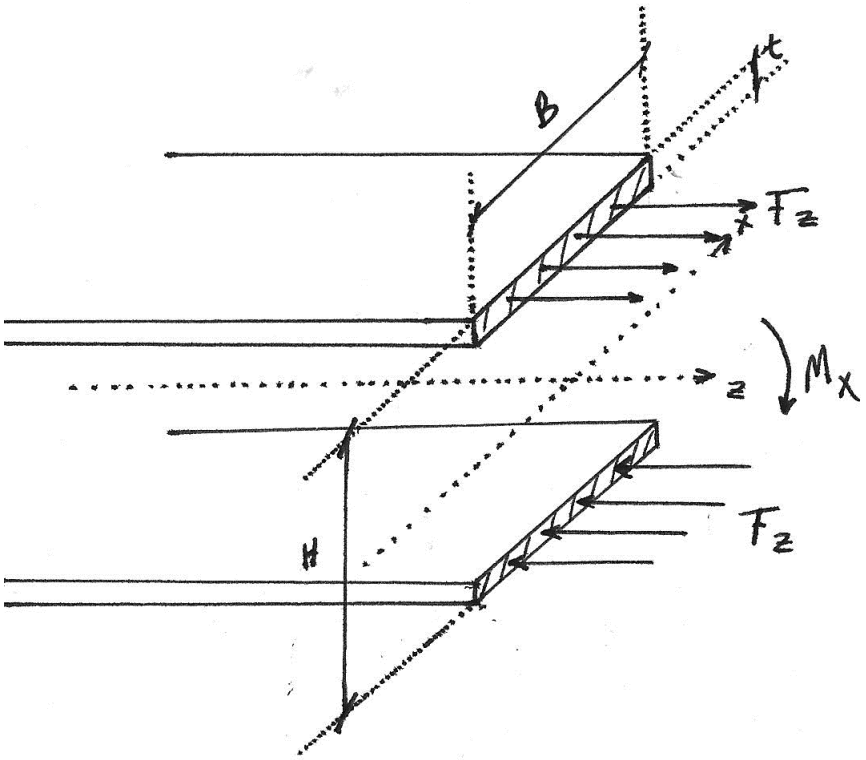

Figure 2.4: Forces acting on the beam due to applied moment M_x

t1

The F_z becomes negative (tensile) and positive (compression) respectively for the upper and lower cap cros-section. To calculate the force, the Eq.2.17 can be used.

$$F_z = \pm \frac{M_x}{H - t} \tag{2.17}$$

From the forces, the local elongations or compressions can be calculated via:

$$\begin{bmatrix} N_z \\ N_y \\ N_{zy} \end{bmatrix} = \begin{bmatrix} A_{11} & A_{12} & A_{16} \\ A_{12} & A_{22} & A_{26} \\ A_{16} & A_{26} & A_{66} \end{bmatrix} \begin{bmatrix} \varepsilon_{z0} \\ \varepsilon_{y0} \\ \gamma_{zy0} \end{bmatrix} + \begin{bmatrix} B_{11} & B_{12} & B_{16} \\ B_{12} & B_{22} & B_{26} \\ B_{16} & B_{26} & B_{66} \end{bmatrix} \begin{bmatrix} \kappa_z \\ \kappa_y \\ \kappa_{zy} \end{bmatrix}$$

Since the curvatures are assumed to be zero, ε values can be calculated easily with *backslash* solver on A matrix via Matlab.

To find the local stresses, the elongation values can be multiplied with the corresponding stiffness matrices which will provide local stresses.

$$\begin{bmatrix} \sigma_z \\ \sigma_y \\ \sigma_{zy} \end{bmatrix} = [Q] \begin{bmatrix} \varepsilon_{z0} \\ \varepsilon_{y0} \\ \gamma_{xy0} \end{bmatrix}$$

2.1.3 Buckling

The buckling response force F_z is calculated as shown below [1].

$$F_z(a,m) = \pi^2[D_{11}(\frac{m}{a})^2 + 2(D_{12} + 2D_{66})\frac{1}{b^2} + D_{22}(\frac{1}{b^4})(\frac{a}{m})^2] \tag{2.18}$$

where a is the plate length, m is the mode number, in other words the amount of half waves, b is the plate width and D is the matrix from ABD for each plate. The equation is applied separately on each plate with varying the longitudinal length in order to find the smallest buckling response.

2.2 Methodology and Results

With the given moments, the first aim was to be able to get max deflection of 12 meters at the tip. The moment distribution is shown in the Fig2.5 through the blade or in other words, beam.

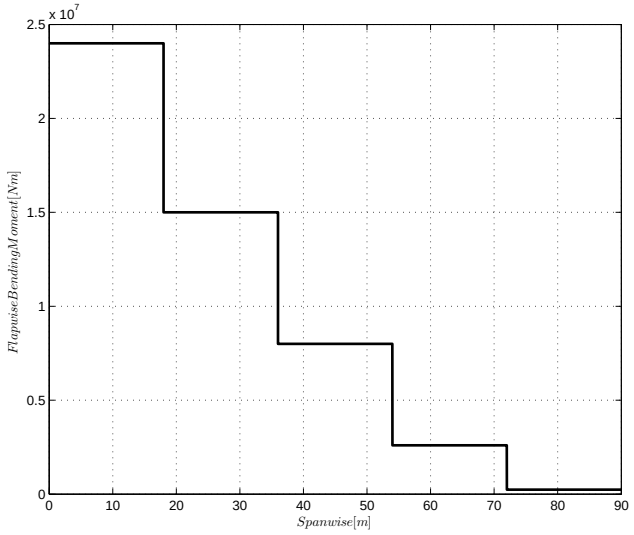

Figure 2.5: Given moment distribution

To achieve this, the configuration shown below in TableB.1 is used.

Section No	Cap thickness [mm]
1	30
2	55
3	75
4	55
5	20

Table 2.1: Very first approach, cap thicknesses

With this configuration, the maximum tip deflection was $11.48m$. The deflections on the beam are shown in the Fig.2.6.

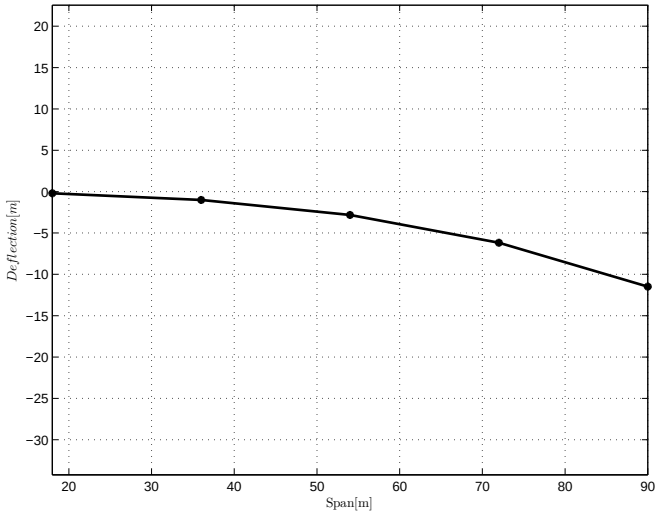

Figure 2.6: Deflections on the beam

After this point, buckling and failure criteria were checked. In order to do this, as explained in the *Theory* section, the moment values on each cross-section represented as tensile and compression forces (see the Fig.2.4).

The moment on each section represented as compression and tensile forces on z-axis. The detailed description is shown in the Fig.2.4. The local elongations or compressions are calculated via ABD matrices where each cap region is assumed to be a plate.

The failure limits of the uni-directional glass-fiber material is shown below.

Direction / stress type	Maximum Value [MPa]
σ_{1t}	900
σ_{1c}	660
σ_{2t}	40
σ_{2c}	60
τ_{12}	60

Table 2.2: Allowable stress limitations

As can be seen from the maximum stress values, the glass-fiber material is more likely to fail under compression load. Since the forces are distributed equally between lower and upper cap regions, the tensile side, in other words the upper cap region, is considered not to fail before the lower region where the main stress would be a compression and the magnitude would be equal with the upper side.

With respect to this issue, the stresses acting on the lower (suction side of the blade) cap region are found and shown in Table2.3.

Stress Type	Sect.1 [Mpa]	Sect.2 [Mpa]	Sect.3 [Mpa]	Sect.4 [Mpa]	Sect.5 [Mpa]
σ_1	170.2	143.5	92.9	66.7	25
σ_2	0	0	0	0	0
τ_{12}	0	0	0	0	0

Table 2.3: Stress distribution on the suction side of the blade

The Matlab code for this calculation can be found in the AppendixA.1.

For long structures, although it sounds innocent, the buckling becomes the main design parameter instead of the maximum stress or strain failure criteria. Therefore, it was considered that buckling would be the main design parameter. Hence, in order to decrease the iterations, the buckling check was done before the failure check.

To check the buckling response, each section is treated separately via Equ.2.18 with varying the plate length in order to be able to catch the lowest buckling response.

The results are shown below. As can be seen from the table, in this approach, the buckling response for sections 1 and 2 were lower than the occurring force. Thus, buckling would be expected.

	Section 1	Section 2	Section 3	Section 4	Section 5
Buckling Response [MN]	0.68	4.76	21.67	15.45	2.75
Acting Force [MN]	5.1	7.1	6.5	3.3	0.5
Thicknesses [mm]	30	55	75	55	20
Cumulative deflections [m]	0.19	0.99	2.82	6.17	11.49 *(tip)*

In order to decrease the acting forces, the thicknesses are increased. With this iteration the new results are shown below in the Table2.4.

	Section 1	Section 2	Section 3	Section 4	Section 5
Buckling Response [MN]	0.68	4.76	21.67	15.45	2.75
Acting Force [MN]	5.1	7.2	6.4	3.3	0.5
Updated thicknesses [mm]	74	73	59	40	15
Buckling index values	0.4979	0.4891	0.4968	0.4159	0.4272
Cumulative deflections [m]	0.0807	0.5591	2.1002	5.6222	11.9185 *(tip)*

Table 2.4: Updated thickness values to avoid buckling

Both thickness configurations are plotted in the Fig.2.8. Simply, the root regions became thicker and mid regions became thinner compare to the first configuration. Moreover, as seen from the Table2.4 the safety factor for buckling is taken to be lower than 0.5. The total tip deflection was also below the limit. The difference in the total deflections can be seen from Fig.2.7.

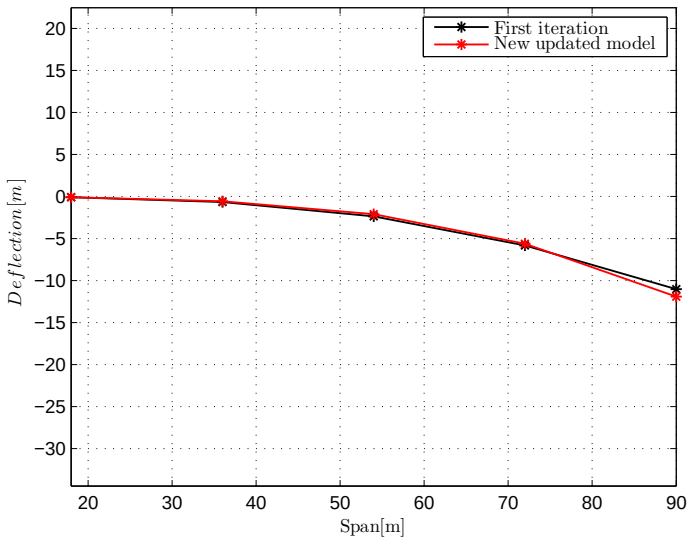

Figure 2.7: Deflections on the beam in comparison to the previous configuration

The matlab code for buckling calculation for each section under different plate lengths, is provided in AppendixA.1.

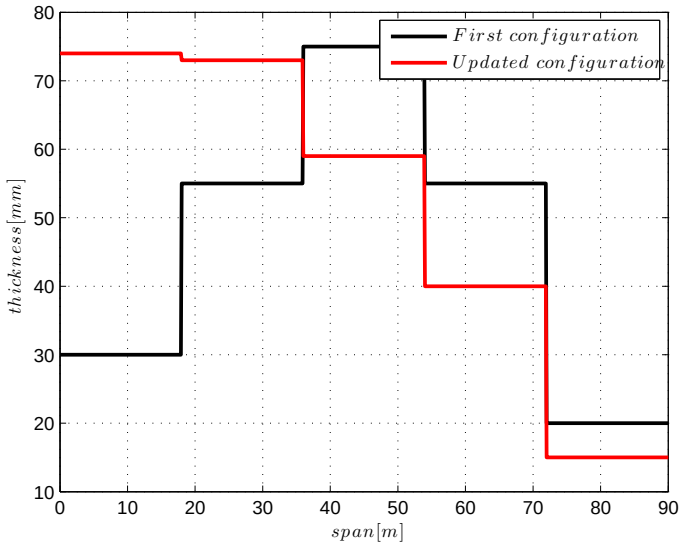

Figure 2.8: Thicknesses from the first and the last configuration

At the end, maximum strain and Tsai-Wu failure criteria were applied to see if the structure was safe enough. In order to find maximum strain values, the relatiosn shown below in Table2.5 are used.

$\hat{\varepsilon}_{1t}$	$\hat{\sigma}_{1t}/E_1 = 0.0214$
$\hat{\varepsilon}_{1c}$	$\hat{\sigma}_{1c}/E_1 = 0.0157$
$\hat{\varepsilon}_{2t}$	$\hat{\sigma}_{2t}/E_2 = 0.0040$
$\hat{\varepsilon}_{2c}$	$\hat{\sigma}_{2c}/E_2 = 0.0060$
$\hat{\gamma}_{12}$	$\hat{\tau}_{12}/G_{12} = 0.0150$

Table 2.5: Lamina strength properties

From the calculations, the indexes shown below are found from Tasi-Wu and maximum strain failure criteria. For Tsai-Wu calculations, F_{12}^* was taken to be 0 which affects the slope of the boundaries of the criterion [3].

	Section 1	Section 2	Section 3	Section 4	Section 5
Maximum Strain	0.1055	0.1506	0.1655	0.1247	0.0500
Tsai-Wu	0.0200	0.0235	0.0240	0.0218	0.0115

Table 2.6: Failure indexes

The requirement was to have safety factor lower than 0.5 for each of these criteria which is clearly satisfied. The matlab code for this calculation is given in AppendixA.1.

At last, the mass of the beam model was 9.71 tons.

Chapter 3

Detailed Analysis with BECAS

3.1 Introduction

3.1.1 Strength Analysis

Strength analysis of the blade is done with BECAS which is a cross-section analysis tool. The software simply calculates the 2-D stiffness properties of each cross section and solves the whole structure with a beam approach. It is not a FEM tool yet it had been proven that the results were more than satisfying.

For calculation, the 2-D sections of the blade is an input to the software. Moreover, the materials and their configurations are need to be provided to the software in order for BECAS to be able to generate stiffness matrices.

The mat layers have non-zero thickness values and are being lied inside the aerodynamic shell or in other words the blade mold in reality. In order to take this thickness effect into account, the python script called shellexpander is used [6]. In simple words, the script generates 2D mesh layers on the negative surface normal direction based on 2-D cross sectional airfoil data and BECAS uses these mesh points to put the materials in. The script also provides the information for different section regions to BECAS where caps, shear webs, leading edge panels etc. can be defined separately.

3.1.2 Buckling Analysis

For linear buckling analysis, Abaqus software, which is a FEM toolbox, is used. For a specific load case, the blade structure is loaded from corresponding defined reference point or in other words, elastic center where this point is constrained to the cross-sections surface points with a fixed distance constraint. With this way, the load applied on the elastic is being distributed to the surface of cross-section. More information can be found in the paper by Capellaro (2013).

3.2 Methodology

The main aim was to find a material configuration for the 90 meter blade and the main considerations were the total blade mass and the failure index values which are grater than one in the first approach.

The kick start was done with the configuration achieved from the beam assumption. Consideration of failure values for each section and adding more material was the following method.

For material selection, the stresses and their directions are considered in cross-section level. For each step, the behavior of the previous material setup was investigated with Paraview, not only failure indexes, also stresses and strains were checked. From the informations gathered via Paraview, materials were changed or thickness values were adjusted. First material selection for main areas was as shown below in the Fig.3.1.

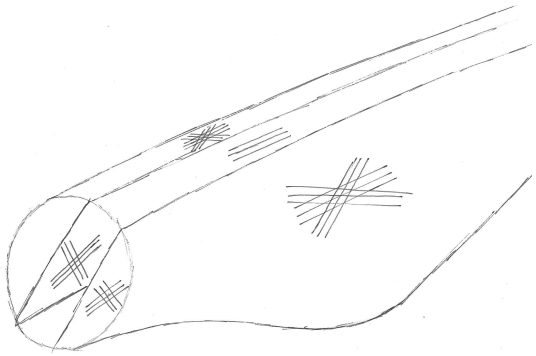

Figure 3.1: First used material configuration on the blade surface

The orientation of fibers are kept on zero degrees. This could be adjusted for instance for constant torsional load coming from the C_m values of airfoil sections, some leading edge triax fiber orientation towards the load direction which could result as better fatigue resistance however, to keep simplicity this wasn't considered for our case.

For failure criteria, maximum strain was considered in order to see in which direction material was failing which was a useful information for correct fiber type selection process.

For the locations where σ_{11} is way higher than other stress components, such as caps and nose, uni-directional fibers are selected. In some regions, although σ_{11} was relatively higher than other components, triax fibers were chosen due to consideration of stress values in second direction and shear stresses acting on the material (e.g. leading, trailing edges).

After the first iteration, nose is handled in a different way. At the beginning, the main idea was to put unidirectional fibers due to occurring high σ_{11} values on edgewise loads.

Nevertheless, with consideration of coupled stress loads observed from Paraview results, triax material was seemed reasonable. However, the decision was to have two layers of unidirectional and a single layer of biax material instead. With this setup, the shear stiffness was adjustable without adding more unidirectional fibers which would add unnecessary weight. The shear considered to be high especially at the root section due to occurring torsion via aerodynamic forces or pitching moments. It has been proven that independent pitch systems are reasonably efficient especially for large rotors such as this one and these systems considered to have relatively rapid pitching movements which would cause high torsion loads due to inertia of the whole blade and could appear as a fatigue damage, if not failure.

The approach for shear webs was straight forward. Shear forces are being handled best with biax material where fibers are oriented at $-45°$ and $+45°$. As a result of this orientation, shear stiffness of these layers are relatively large. Increasing the thickness values if failure was the case was the way which was being followed until the buckling step.

After reaching failure indexes lower than one, the aim was to step to the buckling analysis. The simulations were done under given load case which had sectional lift and drag values inside. With a Matlab script being developed during this process, these force values are distributed along the blade with interpolations on to the existing reference points' elastic centers in each cross-section where the surface nodes were constrained. The code is shown in AppendixA.1. The constrain vectors for a cross-section are shown in the Fig3.2.

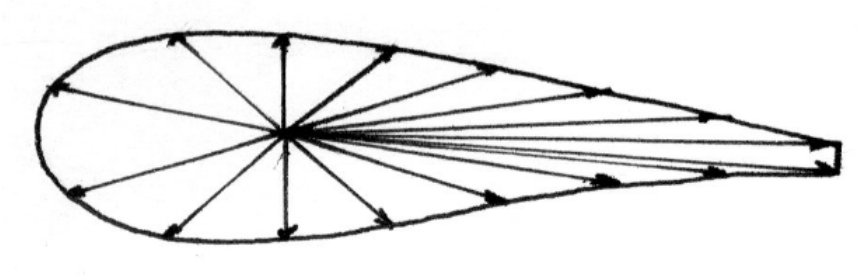

Figure 3.2: Drawing for constraints for each node on the surface point

As seen from the figure, the reference points are connected to the surface nodes with constant distance rule where the load acting on the reference point was distributed with this way.

As explained before, the given load was distributed through the reference points with interpolations yet the coordinates for these reference points we have in structural design were not as same as the ones that used as control points from the HAWC2 model. As a result of this, total moment could vary due to changed so to say 'z' axis coordinate. Before the analyze, the total moment was checked at the root region and it was slightly

higher which wasn't a problem since the blade would still be in the safe side.

With respect to the results achieved from Abaqus simulations, core material injection part was started. Before adding cores, a selection was made between PVC foam and BALSA wood. Considering their material properties, it was concluded that balsa has less stiff structural properties which makes the material more flexible hence it would be harder for balsa to fail due to maximum stress or strain in comparison to PVC foam as a result of having less stresses due to lower E_1 value. As can be seen from Table3.1, balsa is a so to say 'softer' material. In other words, it was seen that PVC's maximum elongation limit in direction 1 was lower than the uni-directional fibers which means that PVC could fail before fiber failure however this is not the case for balsa. To compare, ϵ_{1t} values for balsa, pvc foam and uni-directional fiber material are $9.1000E-02$, $8.5852E-04$ and $9.5230E-03$ respectively. Therefore, to increase the bending stiffnesses of surface panels to add more buckling resistance, balsa wood is used as a core material.

	$BALSA$	$PVCFOAM$
E_1	$5.0000E+07$	$7.2800E+08$
E_2	$5.0000E+07$	$7.2800E+08$
E_3	$2.7300E+09$	$7.2800E+08$
G_12	$1.6670E+07$	$2.8000E+08$
σ_{1t}	**4.5500E+06**	$6.2500E+05$
σ_{1c}	$5.0500E+06$	$1.0500E+06$
σ_{2t}	$3.5000E+05$	$6.2500E+05$
σ_{2c}	$2.0000E+05$	$1.0500E+06$
σ_{12}	$1.0000E+06$	$5.2500E+05$
ϵ_{1t}	**9.1000E-02**	$8.5852E-04$
ϵ_{1c}	$-1.0100E-01$	$-1.4423E-03$
ϵ_{2t}	$7.0000E-03$	$8.5852E-04$
ϵ_{2c}	$4.0000E-03$	$1.4423E-03$
ϵ_{12}	$5.9988E-02$	$1.8750E-03$

Table 3.1: Balsa in comparison to PVC Foam

While adding core materials, the thickness values for sections were dramatically increasing. In order to avoid problems, after each step, mesh clearance was checked especially at the tail regions.

The following step was to check for 1^{st} flapwise and edgewise frequencies. Until this point, there were no any adjustments applied on natural frequencies because of the fact that if the blade was not capable of withstanding under the occurring loads, having the required eigen frequencies would not mean more than being played in the hangar. Nonetheless, in the worst case scenario, controller of the turbine could be adjusted to operate in different conditions with respect to the non-expected blade frequencies.

For adjustment part, to increase the required frequency, the corresponding stiffness would be pumped up and to decrease, since removing material could cause failure, just to be safe some more layers will be added close to the tip region to increase the mass. Although this was not a sensible way of decreasing the frequency for a blade which would be produced, can be used to understand the physics and provide the requested characteristic. Whereas the other way, decreasing the stiffness would cause more iterations which no doubts would result the same in terms of frequency and which for sure should be the way of doing this. However, due to processing power limitations and extremely long buckling simulations, this was not considered.

Moreover, the requested 1^{st} flapwise and edgewise frequencies were $0.613Hz$ and $0.959Hz$ respectively with $\pm 10\%$ flexibility. For design, the aim was to to hit the lower limit in order to have the requested frequency under operating conditions where increased frequencies were seen in many applications due to occurring centrifugal forces and blades behave, so to say, 'more stiff' in terms of vibrations and maximum tip deflections under the same aerodynamic loads.

At the end, the last check was conducted on tip deflections. If any excessive displacements were occurred, increasing cap region thicknesses would solve the problem yet this was not the case for this blade after the rough iterations on buckling steps.

Overall, at the beginning, between the root and 4^{th} meter is considered to have some extra thicknesses for bolts which will carry the whole blade and could generate some local extreme stresses yet due to lack of information, this fact is disregarded.

To stick the spar box, which planned to be built separately and glued to the suction and pressure parts of the blade, glue mat was considered to be used at the beginning. However, as can be seen from the Table3.2, if we assume that these two layers will move to gather where their elongations would be the same, failure will occur in the glue layer due to lower elongation capability before it does in fibers.

	$UNIAX$	$GLUEMAT$
E_1	$4.1630E+10$	$2.0000E+09$
σ_{1t}	$3.9644E+08$	$5.0000E+06$
ϵ_{1t}	**9.5230E-03**	**2.5000E-03**

Table 3.2: Updated thickness values to avoid buckling

After all, considering the smashed glue pieces on the floor from DTU's static blade failure test which was conducted some months ago in Risoe, the whole blade is chosen to be build with one-shot vacuum infusion as Siemens does. Although the blade is extremely big, the infusion process can be modeled with another 3rd party tool and one-shot production can be conducted. Due to this decision, there were no usage of glue or any other kind of adhesive material in the blade.

The results and more detailed comments are provided in the next section.

3.3 Results

After the very first approach with BECAS, it was concluded that the cap region thickness distribution was acceptable with the values taken from the beam model. Nevertheless, in order to decrease the weight some adjustments were applied.

To have simplicity, the blade is designed as if there were no buckling exists at the beginning. Main shear webs are considered to have biax material without core, tail region and leading and trailing edges are filled with triax fibers where tail would have longitudinal loads under edgewise loads but flapwise loads would cause some little shear also in the small web. This is also the case for leading and trailing edges via torsional loads and high torsional stiffness will result with low twist angle variety in torsional modes where the magnitude of the movement in these eigen modes would directly be related to the torsional stiffness values of the blade. This is considered as an important parameter for this long blade where small angle of attack changes would result as huge load differences on the blade surface.

The first reasonable configuration is given in the AppendixB.1.

The strength results can be seen from Fig.3.3

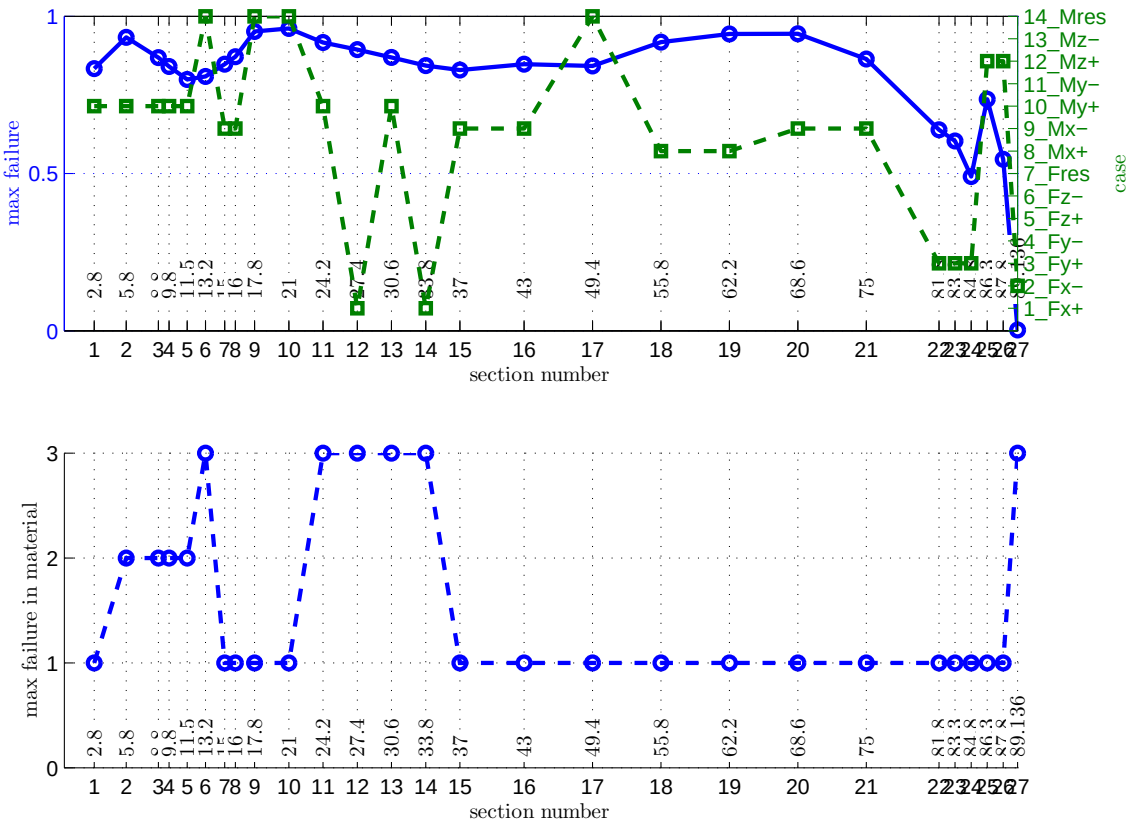

Figure 3.3: Strength results of the first approach

In this case, tip displacement was 9.76 meters and the total mass was just above 28 tons with 95120 units of cost.

In terms of frequencies, although the flapwise frequency was in the limits with $0.68Hz$, the edgewise frequency was way below than the requirement, $0.62Hz$. This could be increased directly with some UD material in the nose and tails and also some to trailing edge however this was planned to be considered at the very end.

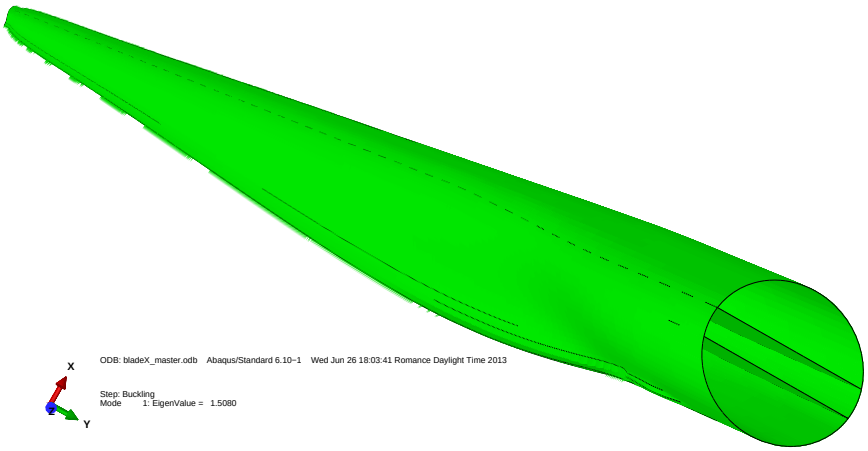

Figure 3.4: Coordinate orientations and 3D layout of the blade

After this point buckling analysis were conducted. The given loads for buckling check are shown in Fig.3.5.

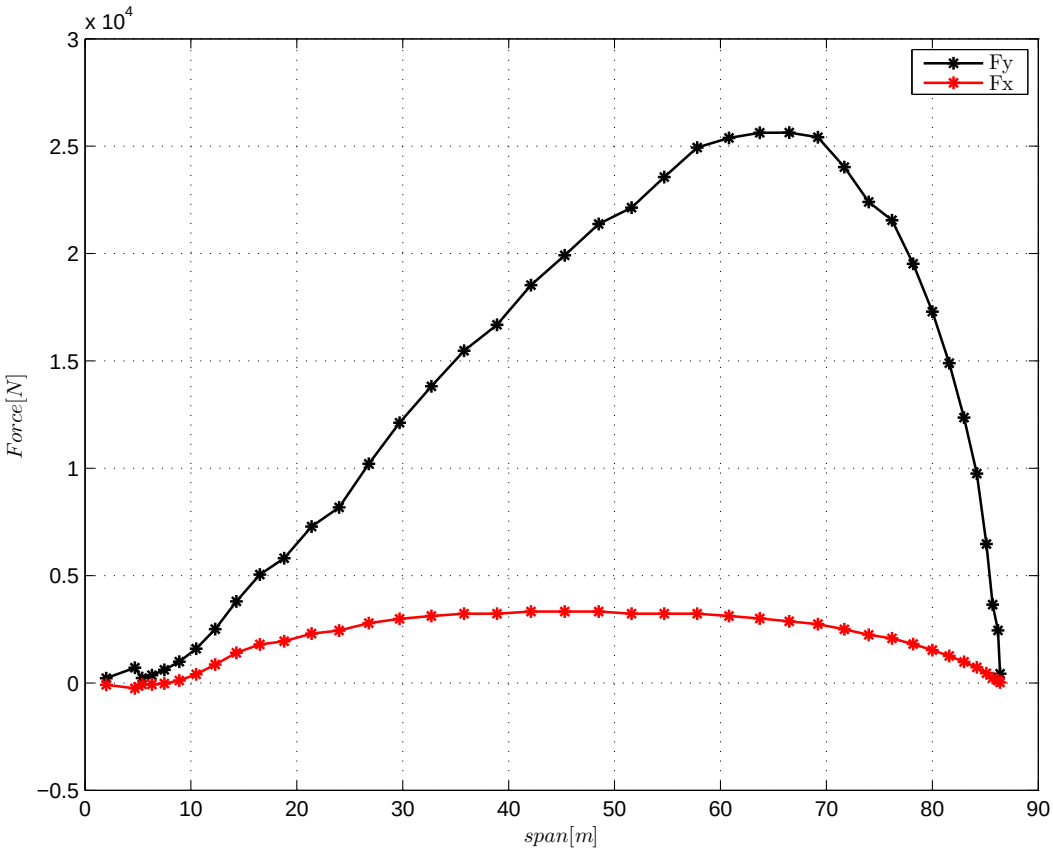

Figure 3.5: Buckling loads

In the first iteration, the buckling response was unsatisfying and was occurring in the main shear webs at very close to the root section where the thicknesses were extremely small. The behavior in 1:1 scale is shown below.

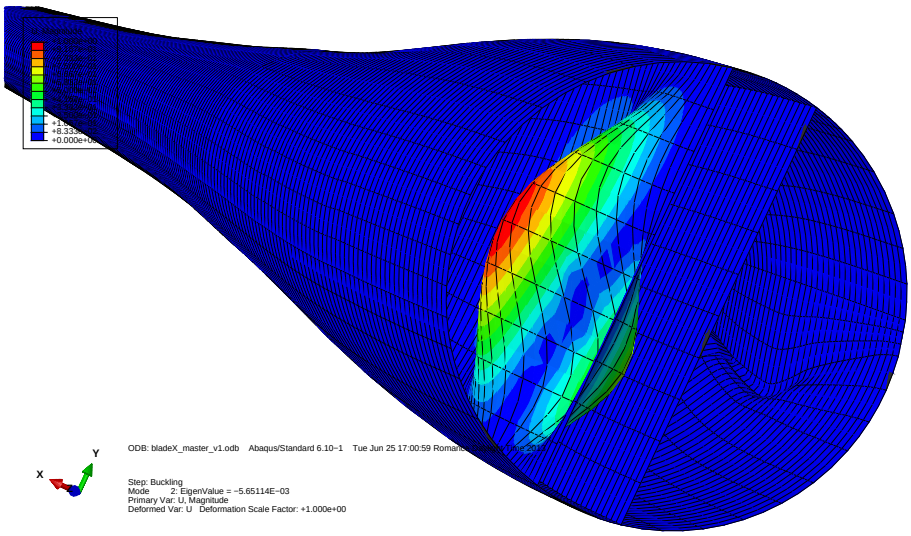

Figure 3.6: Buckling response,shear webs

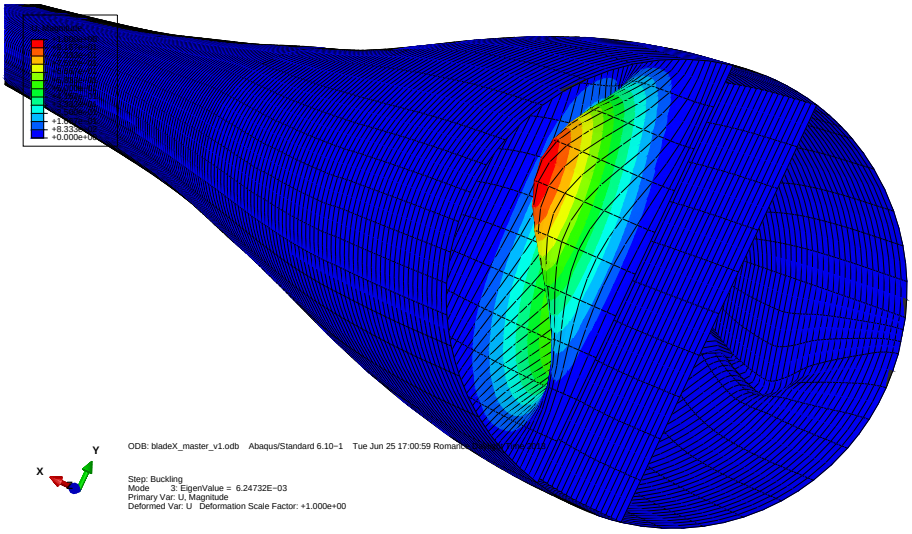

Figure 3.7: Buckling response,shear webs

With respect to the simulations, the buckling occurred at 0.5% of the applied load. After this point shear webs were filled with biax and core material.

After some iterations, the blade showed buckling response index greater than one. Some other buckling failure figures can be seen in AppendixC.

At the end the blade was able to withstand the given load with being buckled (see the Fig.C.4) yet the edgewise frequency was needed to be adjusted. In order to increase the edgewise frequency from 0.7 to around 0.85, some unidirectional material was added to tail and nose regions. As a result of this, the flapwise and edgewise frequencies were $0.57Hz$ and $0.85Hz$ respectively which were at the lower limit of the requirement. As explained before, with consideration of the fact that centrifugal forces will add more stiffness to the blade, these frequencies kept at the lower limit where the operation conditions are expected to increase them to the optimum value. Especially for variable speed machines, this fact needs to be taken into account in the blade design process.

With the last setup, the maximum tip deflection was 7.95 meters which was below the limit, and maximum failure criteria value was 0.85 (see the Fig.3.8). The total cost of the blade was 505.1 thousand cost units.

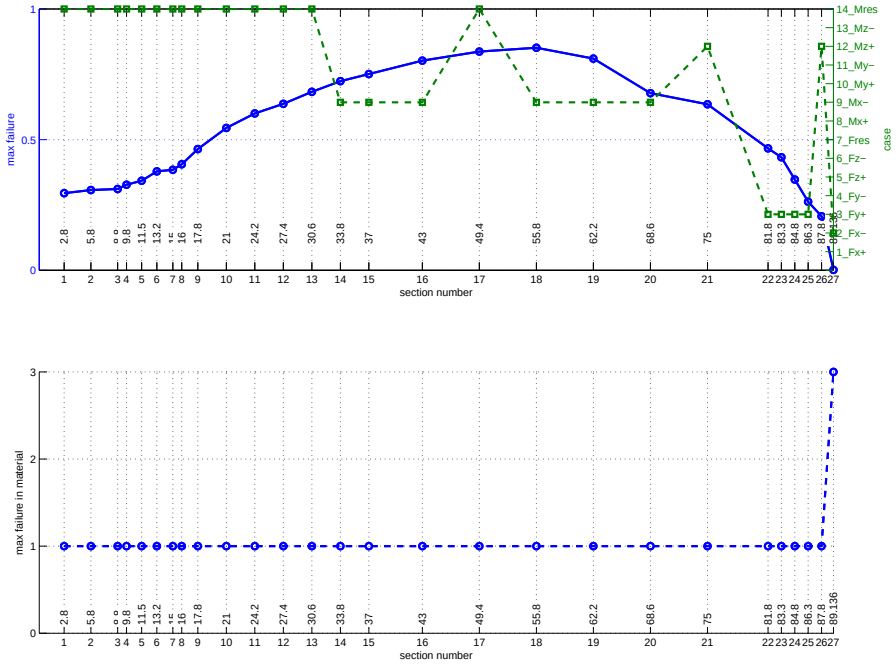

Figure 3.8: Strength results of the last blade

For this configuration one last buckling analysis was run and the result was satisfying where the blade buckled under the force which was 1.5 times grater than the required one (see the Fig.3.9) and the buckling were occurring at the tail region. Nevertheless, the total mass, which was 76658 kg considered to be extremely high. In comparison with Vestas's 3MW nacelles, which are known to be around 70 tons, this single blade is even heavier.

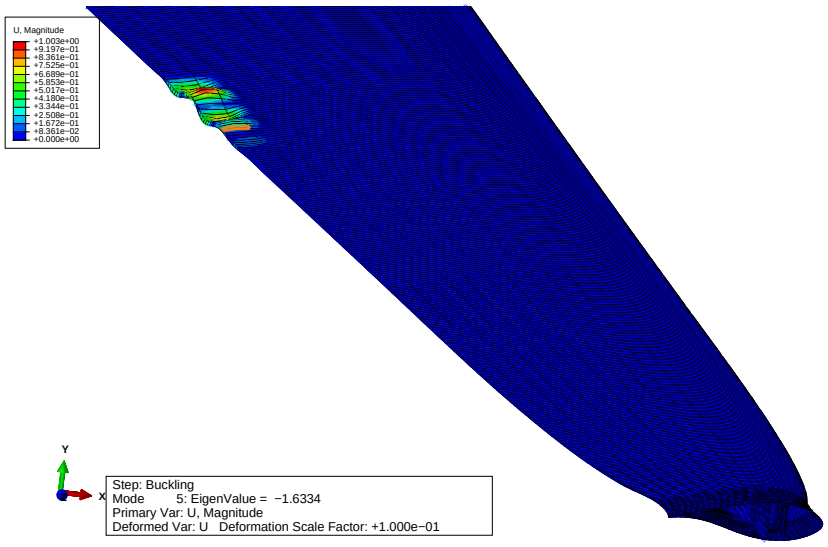

Figure 3.9: Strength results of the very last blade

The last configuration's layup details can be found in AppendixC.2.

Chapter 4

Discussion

4.1 Conclusions

The main conclusion from this report was the good agreement between the beam assumption or in other words, hand calculation and sophisticated models. Simply it was obvious that beam model gives reasonable results. This is visible in the Fig4.1.

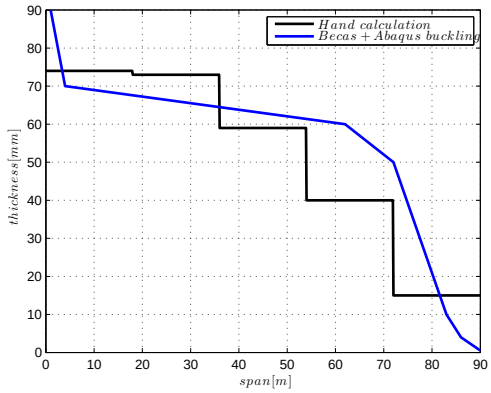

Figure 4.1: Cap region thickness distribution, Beam vs BECAS+Abaqus

On the other hand, the last configuration is considered relatively heavy thus less material in cab region would be sensible where the agreement will improve even further.

Apart from overall view, when we look at the cross-sections, although there were no any mesh or overlapping problems in the BECAS figures (see the Fig4.2), it was obvious that there were some areas where fiber thickness would easily be chopped.

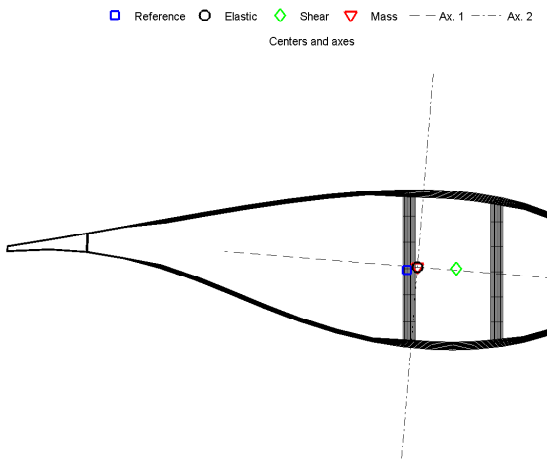

Figure 4.2: Cross section plot from BECAS

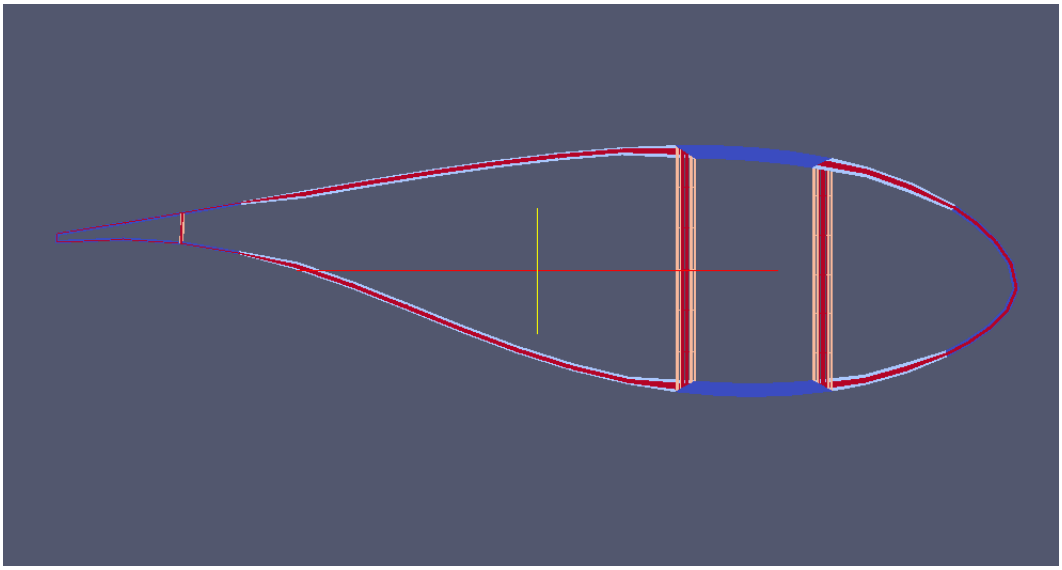

Figure 4.3: Cross section plot via Paraview

As can be seen from the Fig.4.3 the sandwich structures has relatively thick fiber layers in comparison with other application examples. The sandwich structure usage was for increasing the bending stiffnesses, or in other words, values of D matrix. Yet, it was proven in the previous report that instead of adding more fiber material, generating distance between the layers would be more beneficial in terms of bending stiffnesses, cost and of course the mass[3]. The fiber material here was employed to carry the load and the core material was for buckling resistance however due to rough iterations on

buckling steps, excessive usage of fiber material is occurred. As a result of this the total mass became unacceptable.

Apart from these issues, it was seen that specific fiber orientation usage to treat occurring stresses in the 2^{nd} direction may result with failure in 1^{st} direction. At the very beginning, the optimization was started with threating the stress values in layer level. For failure occurring in the second direction, some 90 degree oriented UD fibers were employed to handle that. Nevertheless, while threating that 90 degree fibers were started to fail in the main first direction due to low elongation capability in their second direction. After this point it was concluded that the curing is not straight forward.

Moreover, although it was pretty easy to generate buckling master files for corresponding input with the developed Matlab script (see AppendixA.1), the buckling analysis were excessively time consuming. As a result of this, the mass of the blade couldn't be decreased due to long iteration steps and pretty rough increments on thicknesses to treat bucklings. A lighter and still a safe blade would require a better RAM and CPU configuration. It was observed that the equations running behind the Abaqus were consuming more than 1.4 giga bytes of ram which was also the available amount yet cpu load was falling behind which can be related that ram memory was the main limitation for these calculations. It can be said that with an 8 core i7 processor and 8 gigabytes of ram, linear buckling analysis would surely be solved in less than half an hour for this specific blade with this many mesh nodes.

In general, the BECAS tool was useful and pretty rapid in terms of calculations. The understanding on fiber failures was significantly increased in a short time due to fast observed results. However, at the end of the BECAS work, the blade was around 28 tons. In comparison with the reference blade which was 40 tons, it was obvious that buckling was the main design parameter on reference blade. Thus, it was concluded that BECAS software is unfortunately not yet enough to design a blade for given loads.

Lastly, no doubts the last blade structural configuration was able to withstand under given load conditions yet its weight is unacceptable for application.

4.2 Future Work

4.2.1 Automated Design

In order to decrease the human power in design process, the kick start of the main structural design can be done by a computer. Simply with a reasonable input and usage of BECAS, a script can be coded to employ the cpu to design the structural configuration of a specific blade under some load cases with BECAS. After giving the first rough input, an iterative loop can be conducted from the script. The loop can run on each region and each section, judge the stresses for each directions, select an appropriate

material with respect to the ratio between stress values and input parameters, change the thicknesses and go to the next iteration step. A simple block diagram is shown below in Fig.4.4.

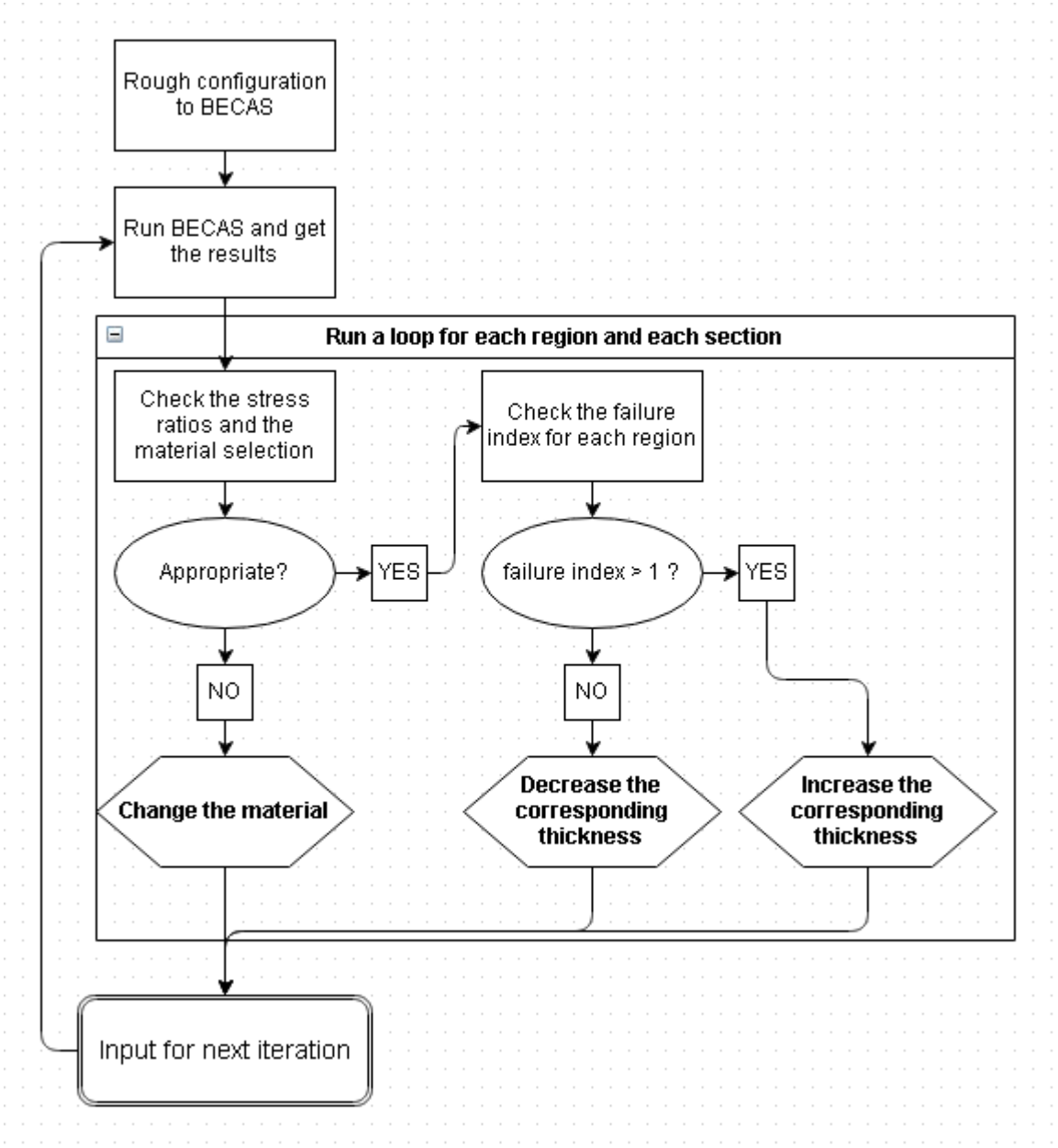

Figure 4.4: Block diagram of a script for an automated blade designer via BECAS

Instead of using fiber composite material, an isotropic material can be used for the first rough input which would provide reliable information to the computer to select an appropriate fiber direction/type.

Although it sounds no-sense, all the knowledge can be coded to a script and even buckle-safe blades can be designed by an automated script with detailed input parameters and

experience.

4.2.2 Buckling resistance

For buckling simulations, the blade can be divided into sections and moments can be applied directly which would save a lot of time. In theory, buckling responses are relatively high for longer plates thus section-by-section simulations would result with good agreements with the full scale analysis.

A coarse mesh could be used on the blade and as a consequence of this, faster iteration steps would be conducted. At the end, a fine mesh could be employed to be able to have more realistic results for tiny adjustments. Moreover, clusters can be used with non-linear buckling analysis would be more realistic if any possible.

For this specific blade, sections can be investigated 1-by-1 and increase in core material thicknesses and decrease in fiber material could be efficient in terms of mass, cost and also buckling resistance.

4.2.3 Fatigue

The fatigue is an important parameter which needs to be considered in the design step.

However, the fatigue prediction for fiber composite materials are very hard to do due to the very small slope they have in their Wohler, or in other words, S-N curves. As a result of this, total life time predictions with rain flow counting can dramatically vary. Yet, this is the only way to predict future for now.

In order to implement this, this blade can be simulated with an aero-elastic code such as DTU's FLEX5 or HAWC2, NREL's FAST or GL Garrad Hassan's Bladed. With an aero-elastic code and proper wind climate input such as IEC Load Cases, whole acting moments can be simulated and recorded for a short period of time with respect to corresponding wind speed. After this point, these captured moments, or so to say 'loads', can be distributed to year with a specific weibull distribution with respect to the climate that the turbine designed for and total life time can be calculated with S-N curves and rainflow counting.

Unfortunately, the reality is not that straight forward. The main issue is, the Wohler (S-N) curves usually represent single directional dynamic loading. For isotropic materials such as aluminum, occurred stress in two directions can be considered as if it was a single directional stress with von-Misses stresses. Nevertheless, for composites, these stresses can not be calculated that easily where the stiffnesses varying a lot between directions especially for uni-directional. Moreover, consider a fiber layer in a turbine blade, carrying some static load, and there is also some excessive dynamical loading acting on it maybe as a result of another turbine's wake coupled with tower shadow and some non-stable atmospheric conditions where the heat fluxes would become excessive.

As a result of this some stresses could occur which were not taken into account at the beginning. When we re-consider the S-N curves, it is obvious that material life time is way more related to occurred stress levels in comparison to the typical metals especially for carbon fibers. Hence, life time would vary a lot and predictions are non-reliable.

Overall, a fiber-glass layer under compression load is more close to failure than a layer under tensile load. This scenario is same for cap regions on pressure and suction side of a wind turbine blade. Simply, either for fatigue or direct failure, the cap region under compression is more close to the failure. Hence, the design of these regions could be made independently.

4.2.4 Production

As clarified in previews chapter, the blade is considered to be built in one-shot vacuum infusion technique. However, root section could become problematic with exothermic heat increase due to very thick regions. In order to avoid this, temperature needs to be checked frequently during the vacuum process. It is better to keep the temperature low yet this would also cause viscosity increase for epoxy material which will slow down the process. On the other hand, although viscosity will drop down with higher temperatures, curing process would kick in and material would loose its fluidity dramatically. If any curing problems occur due to fast cured epoxy, epoxy can be injected afterwards yet this technique would, no doubts, lower the mechanical properties of the composite region.

To avoid problems, a root region could be mimicked and infusion process could be proceeded only for first, so to say, several meters of the blade root part. This test would provide a lot of information to the producer without risking the 90 meter blade.

If exothermic reaction becomes uncontrollable due to slow infusion process, pre-prag layers can be considered. Some big players in the market such as Danish Vestas, use pre-prag technology for their blades where exothermic heat is not as problematic as it is in the infusion techniques.

Apart from this, as mentioned before, bolts were not included in the design. However, these mechanical products are as important as the whole blade since the structure will be carried by them. To take them into account, some T-bolts can be added with FEM simulations to the root section and some extra material can be used to distribute the loads with respect to the occurring aerodynamic loads, pitching torsional and gravitational loads and as well as centrifugal forces.

4.2.5 Final cost

The blade is considered to be built by a team which have knowledge of blade production and with appropriate facilities. Furthermore, the mold is assumed to be ready and

excluded from the total cost. The rough table for work hours is shown below.

	number of workers	day	Man-hour
Placing the mats	15	15	1800
Resin flow channels & vacuum bag app.	15	5	600
Vacuum infusion	50	1.5	600
Last curing with kiln	5	5	200
Painting the surface	3	1	24
Drilling and adding bolts	5	3	120
TOTAL			**3344**

In Denmark where the salary is considered to be DKK150/hour, the manufacturing process of this blade would cost roughly €71.600. At the end blade would become as expensive as 505085 cost units + €71.600.

The wasted fiber materials and mixed epoxy are also excluded from the cost.

Appendix A

Matlab Functions

A.1 Simple Beam

Total tip deflection

```
set(0, 'defaultTextInterpreter', 'latex');
clear all;clc;close all;

E1=42e9;
E2=10e9;
G12=4e9;
nu12=0.28;
nu21=nu12*E2/E1;
H=[4.73 2.14 1.30 0.83 0.5]; % spar heights
b=[1.43 1.17 0.91 0.65 0.39]; % spar cap widths
M=[24e6 15e6 8e6 2.6e6 0.24e6]; %Nm

t=[30 50 70 50 20]*10^-3; % cap UD thicknesses

seq=[0 0 0 0] ; %orientation of layers (all zero in this case)
n=length(seq); %number of layers
% stiffness matrix for UD and mid space
Q1=stiffness2(E1, E2, G12, nu12); %stiffness matrix for UD
Q0=zeros(3,3); %stiffness matrix // represents the space between UD ...
    layers // [H]

%Rotate stiffnesses w.r.t. orientation (zero in this case)
for i=1:length(seq)
    if i == 1 | i==4
    Q(:,:,i)=stiffness_matrix_rotater(Q1,seq(i));
    else
    Q(:,:,i)=stiffness_matrix_rotater(Q0,seq(i));
    end
end

%% run through whole blade for each section
zz=[18 36 54 72 90];
for i=1:length(zz)
%heights of each layer [ start and end points ]
```

```
a1=-(H(i)+t(i))/2 ;
a2=-(H(i)-t(i))/2;
a3=(H(i)-t(i))/2;
a4=(H(i)+t(i))/2;
z=[a1 a2 0 a3 a4];

%Get the ABD
[ ABD,A,B,D ] = ABDgenerator(Q,z,n);
A11(i)=A(1,1);
end

E=(A11.*(1-nu12*nu21))./(2*t); % modulus values for each section
I=((b.*t.^3)/12 + t.*b .*((H-t)./2).^2)*2;
%% calculate the deflections and slopes at each zz point
L=[zz(1) diff(zz)];
y(1)=M(1)*L(1)^2/(E(1)*I(1)*2);
dydz(1)=M(1)*L(1)/(E(1)*I(1));

y(2)=y(1) + M(2)*L(2)^2/(E(2)*I(2)*2) + dydz(1)*L(2);
dydz(2)=dydz(1) + M(2)*L(2)/(E(2)*I(2));

y(3)=y(2) + M(3)*L(3)^2/(E(3)*I(3)*2) + dydz(2)*L(3);
dydz(3)=dydz(2) + M(3)*L(3)/(E(3)*I(3));

y(4)=y(3) + M(4)*L(4)^2/(E(4)*I(4)*2) + dydz(3)*L(4);
dydz(4)=dydz(3) + M(4)*L(4)/(E(4)*I(4));

y(5)=y(4) + M(5)*L(5)^2/(E(5)*I(5)*2) + dydz(4)*L(5)
dydz(5)=dydz(4) + M(5)*L(5)/(E(5)*I(5));
```

Stress calculation

```
%path office
addpath(genpath('C:\Users\s111058\Desktop\Dropbox\...
Fibre_Composites\functions\'));
%path linux
addpath(genpath('/media/kaya/A4A2EEE5A2EEBB46/Users/...
Administrator/Dropbox/Fibre_Composites/functions'));
set(0, 'defaultTextInterpreter', 'latex');
clear all;clc;close all;

E1=42e9;
E2=10e9;
G12=4e9;
nu12=0.28;
nu21=nu12*E2/E1;
H=[4.73 2.14 1.30 0.83 0.5]; % spar heights
b=[1.43 1.17 0.91 0.65 0.39]; % spar cap widths
```

```
M=[24e6 15e6 8e6 2.6e6 0.24e6]; %Nm

t=[30 50 70 50 20]*10^-3; % cap UD thicknesses

seq=[0 0 0 0] ; %orientation of layers (all zero in this case)
n=length(seq); %number of layers
% stiffness matrix for UD and mid space
Q1=stiffness2(E1, E2, G12, nu12); %stiffness matrix for UD
Q(:,:,1)=Q1;
Q(:,:,2)=Q1;
%% run through whole blade for each section
n=2
zz=[18 36 54 72 90];
for i=1:length(zz)
z=[-t(i)/2 0 t(i)/2];
%Get the ABD
[ ABD,A,B,D ] = ABDgenerator(Q,z,n);
AA{i}=A; %save the A matrix
end

%% Fz for each section and region
Fz=M./(H-t)
%% get the stresses
for i = 1:length(zz)
eps(:,i)=AA{i}\[Fz(i);0;0]
sigma(:,i)=Q1*eps(:,i)
end
```

Buckling calculation

```
%% Buckling responses
aa=[zz(1) diff(zz)]; %%length of each plate
m=1; % mode number
for i = 1: length(zz)
    aaa=0.1:0.1:aa(i);
    for j=1:length(aaa)
    %buckling response function
Fzz=@(a,m) pi^2*((DD{i}(1,1)*(m/a)^2) + ...
    2*(DD{i}(1,2)+2*DD{i}(3,3))/b(i)^2 ...
    + DD{i}(2,2)*(1/b(i)^4)*(a/m)^2)
fz(j)=Fzz(m,aaa(j));
    end
    fZ(i)=min(fz);
    %get the index for lenth of the plate
    index(i)=find (fz==fZ(i));
end
%buckling index for each region.
%if greater than 1, increase the thickness
```

```
bi=(Fz/10^6)./(fZ/10^6)
```

Failure Criteria

```
%% max stresses
s1t=900e6; %max stress direction 1 tension
s1c=660e6; %max stress direction 1 compression
s2t=40e6;  %max stress direction 2 tension
s2c=60e6;  %max stress direction 2 compression
s12=60e6;  %max stress direction 12 shear


%% Max Strain
eps_max_1t=s1t/E1;
eps_max_1c=s1c/E1;
eps_max_2t=s2t/E2;
eps_max_2c=s2c/E2;
eps_max_12=s12/G12;
for i =1: length(zz)
%% calculate the index value
    f(i)=eps(1,i)/eps_max_1c
end

%% Tsai-Wu
sigma_max_1t=s1t;
sigma_max_1c=s1c;
sigma_max_2t=s2t;
sigma_max_2c=s2c;
sigma_max_12=s12;

F12_s=0;
F11=1/(sigma_max_1t*sigma_max_1c);
F22=1/(sigma_max_2t*sigma_max_2c);
F12=sqrt(F11*F22)*F12_s;
for i = 1:length(zz)
%% calculate the index value
f_tsai(i)=(sigma(1,i)^2     ...
    /(sigma_max_1t*sigma_max_1c)+sigma(2,i)^2     ...
    /(sigma_max_2t*sigma_max_2c)+sigma(3,i)^2    ...
    /sigma_max_12^2+2*F12*sigma(1,i)*sigma(2,i)+sigma(1,i)/sigma_max_1t-sigma(1,i)/sig
end
```

Buckling analysis with abaqus, master file generator

```
                %%%%%%%%%%%%%%%%%%%%%%%%%%%%%%%%%%%%%%%%%%%%%%%%%
```

```
%%% Abaqus Shell Model Master File Generator  %%%
%%%           for Buckling Analysis           %%%
%%%           with Given Load Input           %%%
%%%%%%%%%%%%%%%%%%%%%%%%%%%%%%%%%%%%%%%%%%%%%%%%

%Simply, reads the mesh file and gets the numb..%
%er of reference points and their coordinates,..%
%reads the load input and transfers the load t..%
%o nearest reference point with a linear inter..%
%polation and generates a master file with req..%
%uested properties and output data.             %

clear all;fclose all;clc;
%%                        ###   I N P U T S   ###
%the input file names
loads='load_data_rich.txt';      % File consist loads inside
abaqus_mesh='blade_mesh3.inp';   % Main abaqus file where geometry ...
    is defined
materials='blade_materials.inp'; % Material configuration file
layup='blade_layup.inp';         % Layup configuration file

%switch for load type
rich_input=1; %switch to '1' for Fx,Fy,Fz,Mx,My,Mz input else '0' ...
    for Fx,Fy

%buckling analysis parameters
no_modes =  5;  % Number of modes      #default = 5
no_vec   = 15;  % Number of vectors    #default = 25
no_iter  = 30;  % Number of iterations #default = 30

%output file name
master_file='bladeX_master.inp';

%%                      ### no need to touch below* ###

%Read the mesh file
FID = fopen(abaqus_mesh, 'r');
if FID == -1, error('Cannot open file'), end
Data = textscan(FID, '%s', 'delimiter', '\n', 'whitespace', '');
CStr = Data{1};
fclose(FID);

search4='** PART INSTANCE: RefPoint-';

indexC = strfind(CStr, search4); %find the line and corresponding ...
    column number
line = find(~cellfun('isempty', indexC)); %get the line number

number_of_ref=length(line); %get the max. number of reference points

% Get z coordinates of the Reference points
```

```
for i = 1:number_of_ref
z_ref(i)=str2num(CStr{line(i)+3,1}(27:38));
end

%Get the requested z coordinates from the loads file
A=importdata(loads); z=A.data(:,1);

%Get the nearest point to apply the load
for i=1:length(z)
ref_no(i)=findnearest(z_ref,z(i));
if i>1; if ref_no(i)≤ref_no(i-1)
            ref_no(i)=ref_no(i)+(ref_no(i-1)-ref_no(i))+1; end;end
end

%Get the corresponding load values for picked reference points
Fy_ref=interp1(z,A.data(:,2),z_ref(ref_no));Fy_ref(isnan(Fy_ref))=0;
Fx_ref=interp1(z,A.data(:,3),z_ref(ref_no));Fx_ref(isnan(Fx_ref))=0;

if rich_input==1
    Fz_ref=interp1(z,A.data(:,4),z_ref(ref_no));Fz_ref(isnan(Fz_ref))=0;
    Mx_ref=interp1(z,A.data(:,5),z_ref(ref_no));Mx_ref(isnan(Mx_ref))=0;
    My_ref=interp1(z,A.data(:,6),z_ref(ref_no));My_ref(isnan(My_ref))=0;
    Mz_ref=interp1(z,A.data(:,7),z_ref(ref_no));Mz_ref(isnan(Mz_ref))=0;
end

% Generate the master file
fid = fopen(master_file, 'w');

fprintf(fid, '%s\n','**************************************');
fprintf(fid, '%s\n','***       Wind Turbine Blade       ***');
fprintf(fid, '%s\n','***    Abaqus Buckling Analysis    ***');
fprintf(fid, '%s\n','***           Master File          ***');
fprintf(fid, '%s\n','**************************************');

fprintf(fid, '%s%s\n','*INCLUDE, INPUT=',abaqus_mesh);
fprintf(fid, '%s%s\n','*INCLUDE, INPUT=',materials);
fprintf(fid, '%s%s\n','*INCLUDE, INPUT=',layup);

fprintf(fid, '%s\n','*ORIENTATION, NAME=BLADEORI, SYSTEM=RECTANGULAR');
fprintf(fid, '%s\n','1, 0, 0, 0, 1, 0, 0, 0, 0');
fprintf(fid, '%s\n','2, 0.0');
fprintf(fid, '%s\n','*ORIENTATION, NAME=TE_GLUE_ORI, ...
    SYSTEM=RECTANGULAR');
fprintf(fid, '%s\n','0, 0, 1, 1, 0, 0, 0, 0, 0');
fprintf(fid, '%s\n','3, 0.0');
fprintf(fid, '%s\n','*BOUNDARY');
fprintf(fid, '%s\n','REFPOINT-001_REFPOINT, 1, 6, 0.0');
fprintf(fid, '%s\n','**');
fprintf(fid, '%s\n','**************************************');
fprintf(fid, '%s\n','*** Buckling');
fprintf(fid, '%s\n','** STEP: Buckling');
```

```
fprintf(fid, '%s\n','**');
fprintf(fid, '%s\n','*Step, name=Buckling, perturbation');
fprintf(fid, '%s\n','*Buckle');
fprintf(fid, '%d%s%d%s%d\n',no_modes,', , ',no_vec,', ',no_iter);
fprintf(fid, '%s\n','**');
fprintf(fid, '%s\n','** LOADS');
fprintf(fid, '%s\n','**');
for i=1:length(ref_no)
    fprintf(fid, '%s%s%s\n','** Name: Load-',num2str(i),'   Type: ...
       Concentrated force');
    fprintf(fid, '%s\n','*Cload');

if ref_no(i)<10;      ix='RefPoint-00';
elseif ref_no(i)<100; ix='RefPoint-0';
else                  ix='RefPoint-';end

    fprintf(fid, '%s%s%s%d\n',ix,num2str(ref_no(i)),'_RefPoint, 1, ...
       ',Fx_ref(i));
    fprintf(fid, '%s%s%s%d\n',ix,num2str(ref_no(i)),'_RefPoint, 2, ...
       ',Fy_ref(i));
    if rich_input==0;
        fprintf(fid, '%s%s%s%s\n',ix,num2str(ref_no(i)),'_RefPoint, ...
           3, ','0');
    elseif rich_input==1;
        fprintf(fid, '%s%s%s%d\n',ix,num2str(ref_no(i)),'_RefPoint, ...
           3, ',Fz_ref(i));
        fprintf(fid, '%s%s%s%d\n',ix,num2str(ref_no(i)),'_RefPoint, ...
           4, ',Mx_ref(i));
        fprintf(fid, '%s%s%s%d\n',ix,num2str(ref_no(i)),'_RefPoint, ...
           5, ',My_ref(i));
        fprintf(fid, '%s%s%s%d\n',ix,num2str(ref_no(i)),'_RefPoint, ...
           6, ',Mz_ref(i));
    end
end
fprintf(fid, '%s\n','**');
fprintf(fid, '%s\n','** OUTPUT REQUESTS');
fprintf(fid, '%s\n','**');
fprintf(fid, '%s\n','*Restart, write, frequency=0');
fprintf(fid, '%s\n','**');
fprintf(fid, '%s\n','** FIELD OUTPUT: F-Output-1');
fprintf(fid, '%s\n','**');
fprintf(fid, '%s\n','*Output, field, variable=PRESELECT');
fprintf(fid, '%s\n','*End Step');
fclose(fid);
```

Appendix B

B.1 Configuration Tables

First Input

Caps										
UNIAX[m]	0.03	0.03	0.035	0.08	0.08	0.07	0.03	0.02	0.001	0.0005
span[m]	1	4	18	30	40	62	72	83	86	90
Shear Webs										
BIAX[m]	0.01	0.009	0.008	0.007	0.006	0.001				
span[m]	1	10	30	40	60	90				
Leading Panels										
TRIAX[m]	0.03	0.02	0.02	0.02	0.018	0.01	0.008	0.007	0.006	0.001
span[m]	1	4	13	15	20	25	30	40	60	90
Nose										
UNIAX[m]	0.004	0.004	0.004	0.005	0.002	0.001	0.001			
BIAX[m]	0.003	0.003	0.003	0.002	0	0	0			
UNIAX[m]	0.004	0.004	0.004	0.005	0.002	0.001	0.001			
span[m]	1	4	6	15	30	40	90			
Trailing Panels										
TRAIX[m]	0.01	0.005	0.004	0.002	0.002	0.003	0.002			
span[m]	1	4	6	15	30	40	90			
Tails										
TRAIX[m]	0.01	0.009	0.008	0.006	0.006	0.006	0.004	0.002		
span[m]	1	4	6	15	30	40	50	90		

Last blade

Caps										
UNIAX[m]	0.09	0.07	0.06	0.05	0.01	0.004	0.0005			
span[m]	1	4	62	72	83	86	90			
Shear Webs A & B										
BIAX[m]	0.03	0.04	0.04	0.04	0.01	0.004	0.001			
BALSA[m]	0.05	0.05	0.05	0.05	0.02	0.007	0.001			
BIAX[m]	0.03	0.04	0.04	0.04	0.01	0.004	0.001			
span[m]	1	10	30	40	60	80	90			
Shear Web C										
BIAX[m]	0.005	0.004	0.003	0.003	0.002	0.001				
BALSA[m]	0.01	0.01	0.01	0.01	0.006	0.004				
BIAX[m]	0.005	0.004	0.003	0.003	0.002	0.001				
span[m]	1	10	30	40	60	90				
Leading Panels										
TRIAX[m]	0.015	0.015	0.04	0.02	0.02	0.02	0.015	0.01	0.009	0.001
BALSA[m]	0.04	0.04	0.01	0.04	0.038	0.035	0.03	0.02	0.015	0.001
TRIAX[m]	0.015	0.015	0.04	0.02	0.02	0.02	0.015	0.01	0.009	0.001
span[m]	1	4	13	15	20	25	30	60	70	90
Nose										
UNIAX[m]	0.02	0.015	0.014	0.01	0.008	0.007	0.004			
BIAX[m]	0.01	0.005	0.005	0.004	0.003	0.0	0.0			
BALSA[m]	0.02	0.02	0.02	0.02	0.018	0.017	0.005			
BIAX[m]	0.01	0.005	0.005	0.004	0.003	0.0	0.0			
UNIAX[m]	0.02	0.015	0.014	0.01	0.008	0.007	0.004			
span[m]	1	4	6	15	30	40	90			
Trailing Panels										
TRAIX[m]	0.02	0.018	0.016	0.01	0.008	0.007	0.006	0.005		
BALSA[m]	0.05	0.05	0.045	0.04	0.03	0.02	0.015	0.01		
TRAIX[m]	0.02	0.018	0.016	0.01	0.008	0.007	0.006	0.005		
span[m]	1	4	6	15	30	40	80	90		
Tails										
TRAIX[m]	0.005	0.003	0.001	0.001	0.001	0.001	0.0	0.0		
UNIAX[m]	0.01	0.012	0.006	0.005	0.005	0.004	0.003	0.002		
BALSA[m]	0.015	0.008	0.007	0.006	0.005	0.004	0.003	0.002		
UNIAX[m]	0.01	0.012	0.006	0.005	0.005	0.004	0.003	0.002		
TRAIX[m]	0.005	0.003	0.001	0.001	0.001	0.001	0.0	0.0		
span[m]	1	4	6	15	30	40	50	90		

Appendix C

C.1 Buckling Figures

C.1.1 Buckling failure @ 3.7% of the whole load

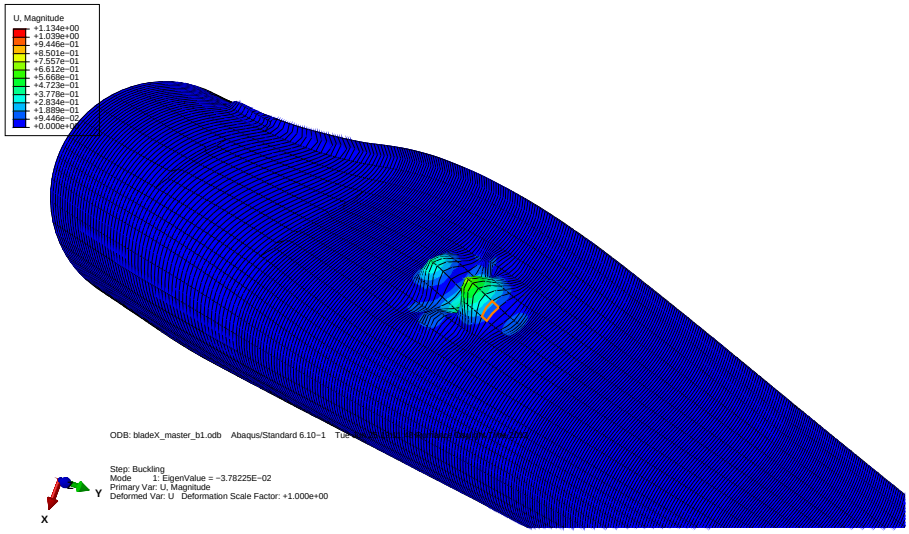

Figure C.1: Buckling response,trailing edge @ 3.7% load

C.1.2 Buckling failure @ 26% load of the whole load

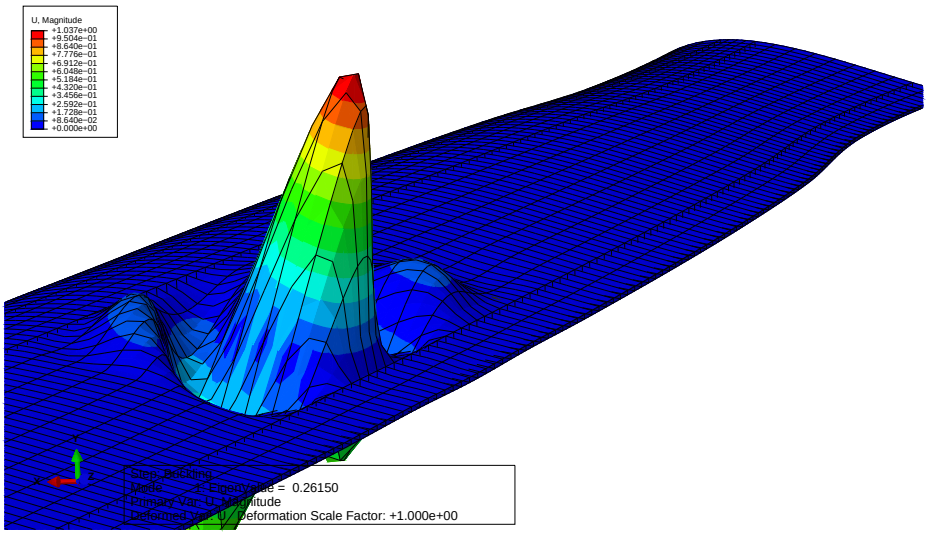

Figure C.2: Buckling response,trailing edge @ 26% load

C.1.3 Buckling failure @ 40% load of the whole load

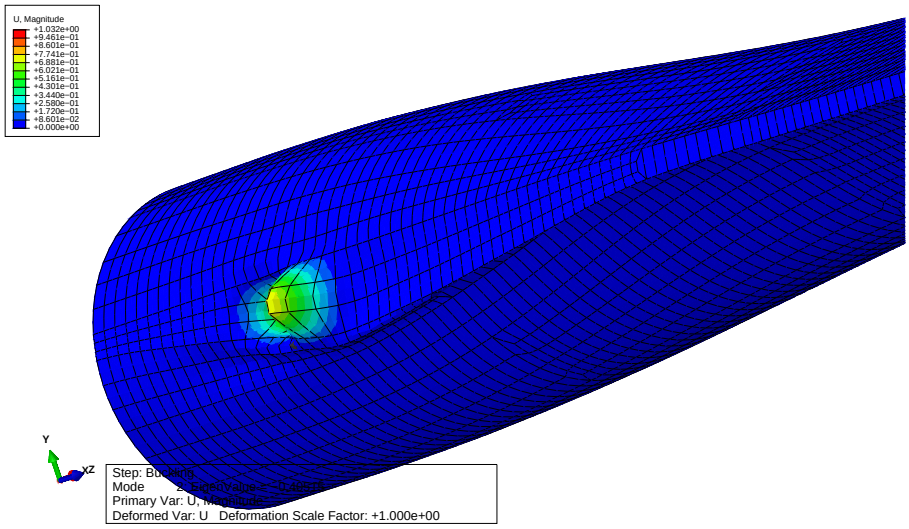

Figure C.3: Buckling response,tail @ 40% load

C.1.4 Buckling response @121% load

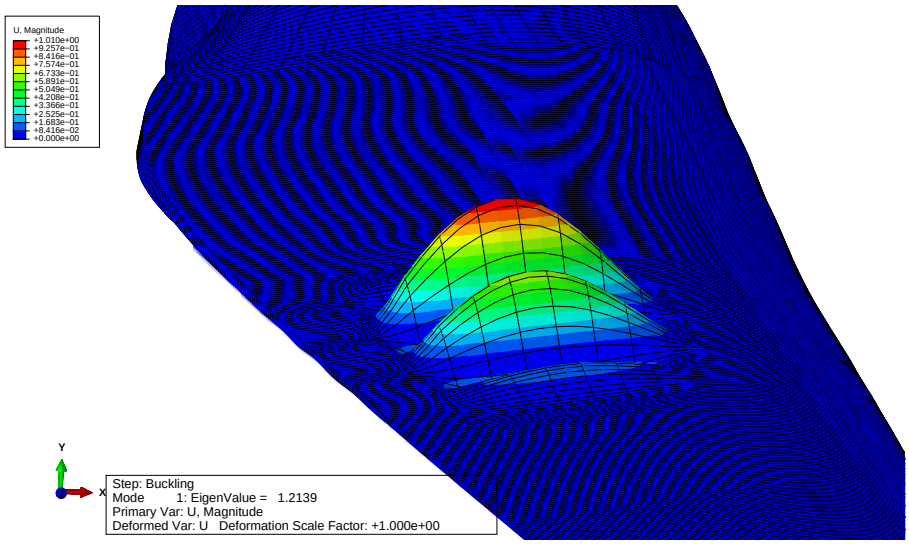

Figure C.4: Buckling response,trailing edge

C.2 Last Material Configuration

C.2.1 Caps

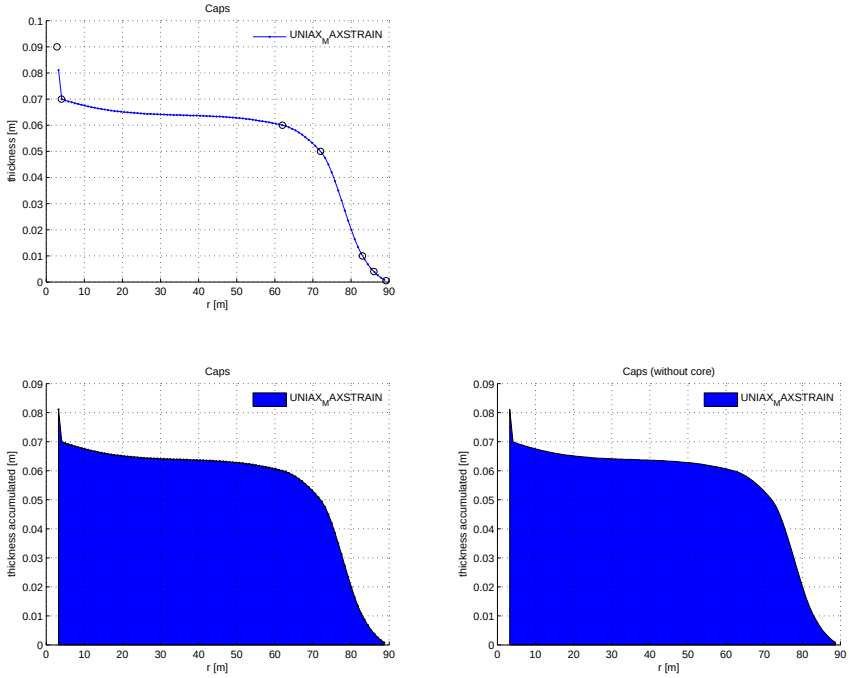

Figure C.5: Cap thicknesses

C.2.2 Nose

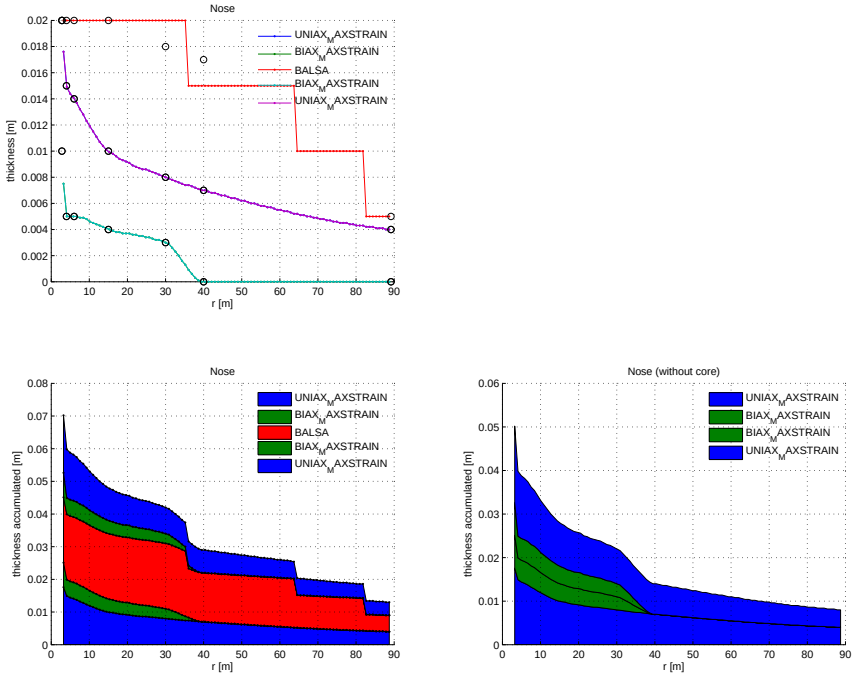

Figure C.6: Nose thicknesses

C.2.3 Leading Edges

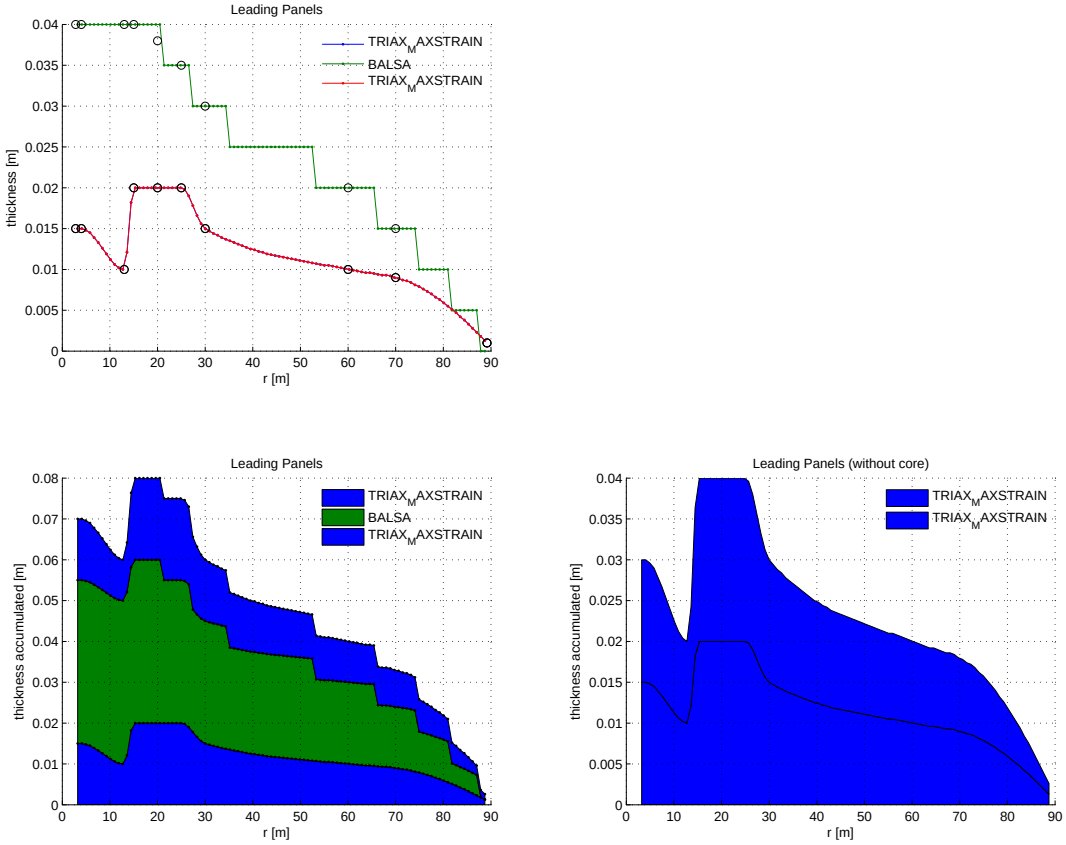

Figure C.7: Leading edge thicknesses

C.2.4 Trailing Edges

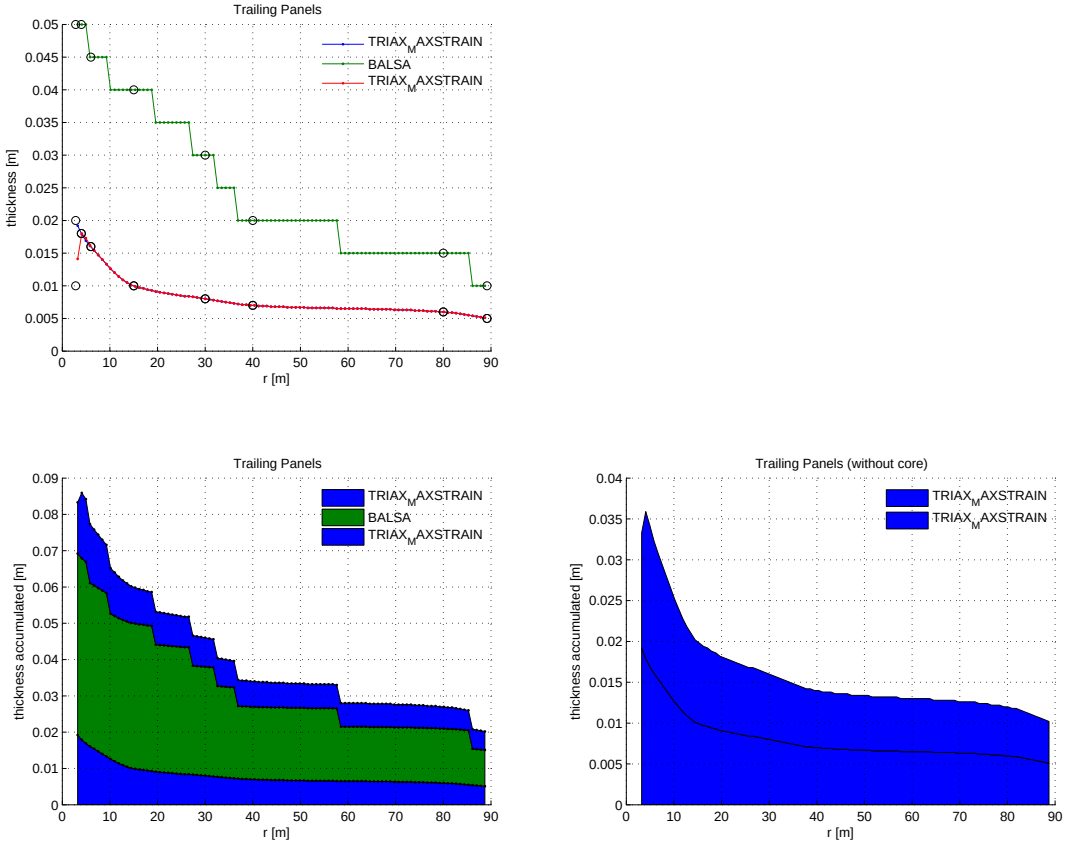

Figure C.8: Trailing edge thicknesses

C.2.5 Shear webs A & B

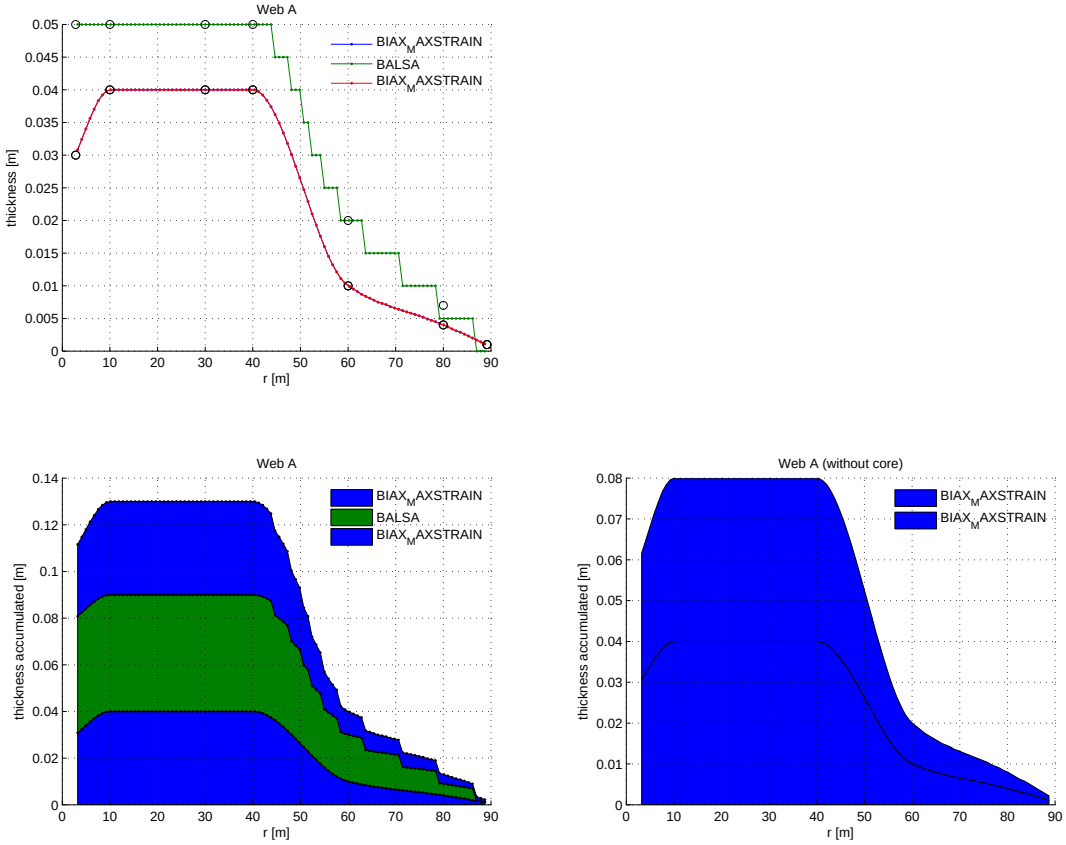

Figure C.9: Shear webs A & B

C.2.6 Shear web C

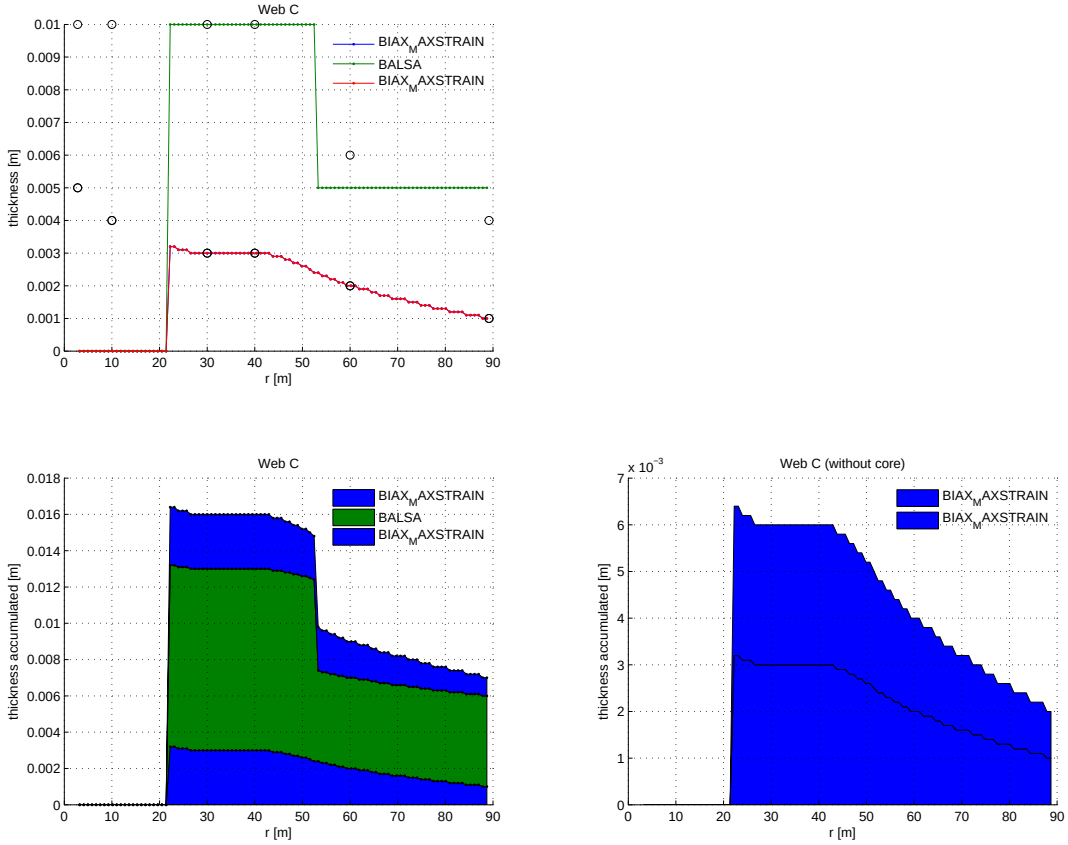

Figure C.10: Shear web C

C.2.7 Tails

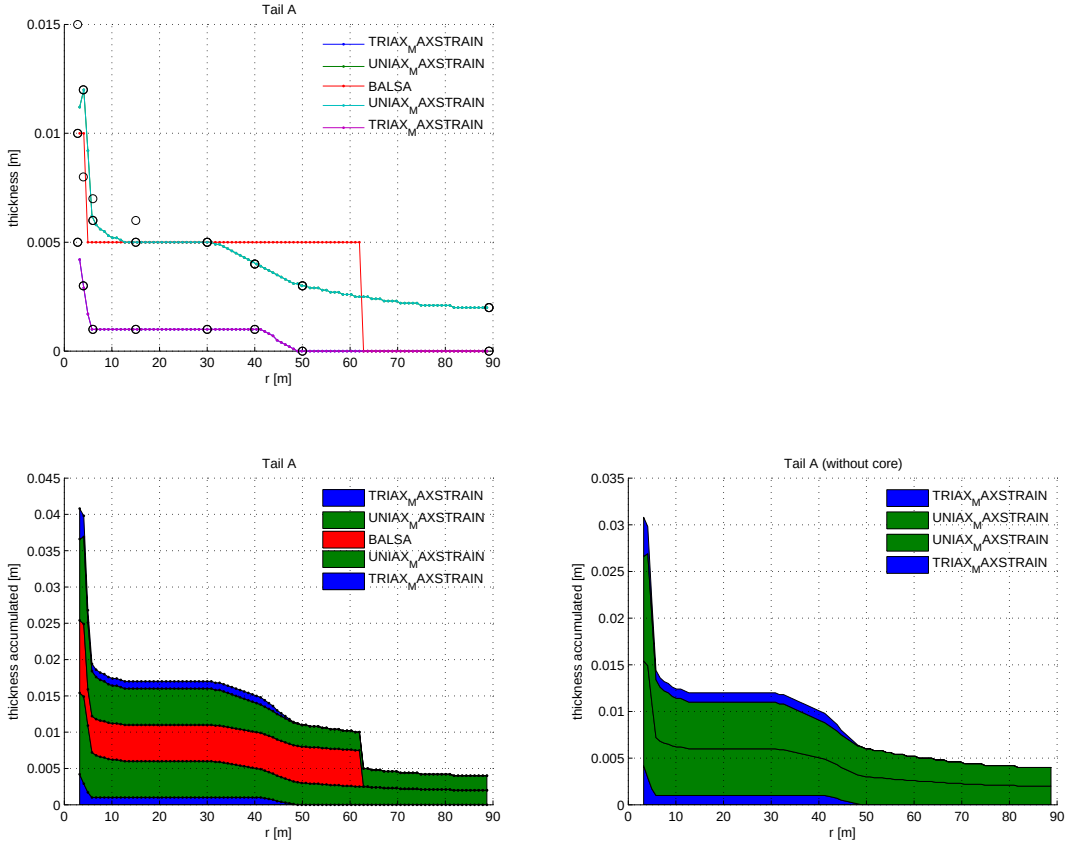

Figure C.11: Tail thicknesses

References

[1] Blasques J. P., Berring P., and Fedorov V. *Designt Project Description Structural Design of the DTU 10MW Wind Turbine*. DTU Wind Energy, May 2013.

[2] Blasques J. P. and Bitsche R. *User's Manual for BECAS*. DTU Wind Energy, March 2013.

[3] Dag K. O. Design of Lightweight Composite Structures Report I. May 2013.

[4] Bucciarelli L. L. *Engineering Mechanics for Structures*. Dover Publications, 2009.

[5] Capellaro M. Three methods for applying aerodynamic loads to a wind turbine finite element blade. May 2013.

[6] Bitsche R. D. *Shellexpander: A preprocessor for the coss-section analysis software BECAS*. DTU Wind Energy, August 2012.